size reduction techniques using shorting wall, shorting pin and the folded patch to obtain small size wide bandwidth microstrip patch antennas

13.1 General Remarks

In many applications, it is desirable for the dimensions of the microstrip patch antenna to be a small fraction of the free space wavelength. The resonant length of the microstrip-patch antenna is approximately $\lambda/2$, where λ is wavelength in the dielectric substrate. It follows that the size of the patch can be reduced by using a substrate material with high dielectric constan. owever, the resulting patch antenna will have narrow impedance bandidth. This motivated the search for other size reduction methods.

By placing a shorting wall along the null in the electric field across he center of the patch, the resonant length can be reduced by a factor of wo. The area occupied by the patch will be reduced by a factor of four, f the aspect ratio is kept the same [1–5]. Another technique to reduce the resonant length is to add a shorting pin in close proximity to the feed [6]. The shorting pin is capacitively coupled to the resonant circuit of the patc., effectively increasing the permittivity of the substrate. It has been shown that a suitably placed shorting pin can reduce the resonant length of a circular patch by a factor of three, and the area of the patch by a factor of ine. Yet another method is to use a folded patch [5–8].

In this chapter, the size reduction techniques using shorting wall, shorting pin and the folded patch are first introduced. The bandwidth broadening techniques using the U-slot, the L-probe and stacked patches are then described to obtain small size wide bandwidth microstrip patch antennas.

13.2 Methods of Reducing the Patch Size

13.2.1 *Use of Shorting Wall — Quarter Wave Patch*

13.2.1.1 *Introduction*

he electric field distributions under the patch for the TM_{01} and TM_{10} odes have a null along the center of the patch. The fields are not perturbed

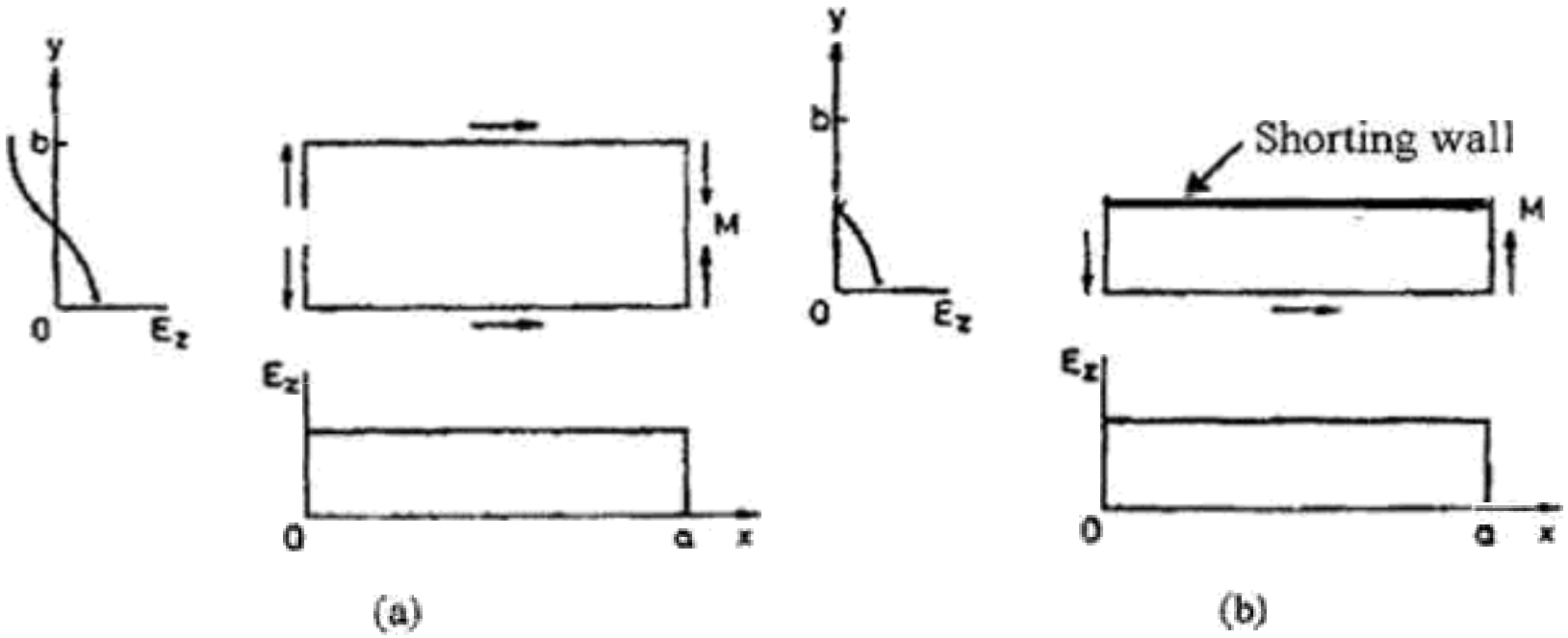

Fig. 13.1 Electric field ibutior of (a) regular half-wave patch and (b) shorted quarter-wave patc...

hen a short is placed at the null line, as shown in Figure 13.1. This results in a shorted qua ter-wave patch, witl :he same resonant frequency as the regular half-wave patch. The area will be half of the half-wave patch if the dimension along x remains the same. If the dimension alo g x is red by half (from a to $a/2$) so that the aspect ratio remains the same as the original patch, the area will be four times smaller.

.2.1.2 *Formula for resonant frequency*

Consider the ectangular cavity epresenting 1 patch shown in igure 13.2, where the side wall $=0$ is shorted. Thus $=0$ $=0$ as

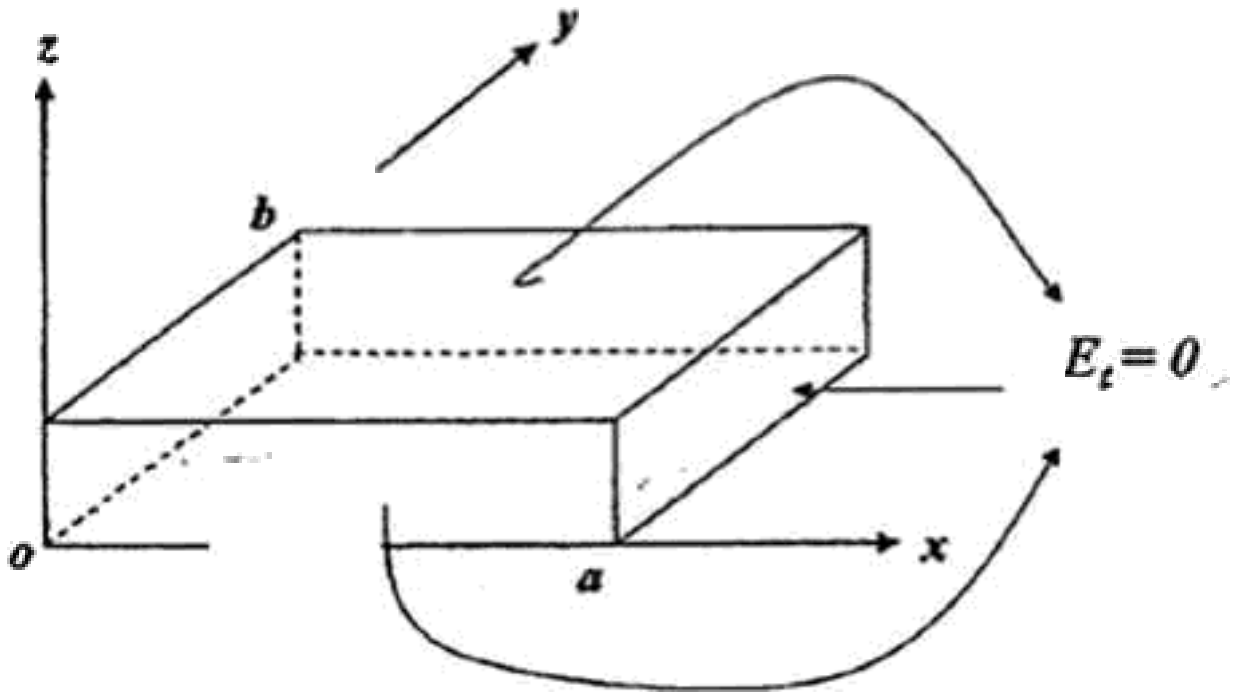

Fig. 13.2 Geometry of the shorted patc

l as on the top and bottom, while $H_t = 0$ on the other three side walls. The solution for $\nabla^2 E_z + k_d^2 E_z = 0$ satisfying the boundary conditions is:

$$E_z = E_0 \cos\left(\frac{m\pi}{a}x\right) \sin\left(\frac{(2n+1)\pi}{2b}y\right) \tag{13.1}$$

he eigenvalues fo k_d^2 are given by:

$$k_{mn}^2 = \left(\frac{m\pi}{a}\right)^2 + \left(\frac{(2n+1)\pi}{2b}\right)^2 \tag{13.2}$$

The resonant requencies are therefore given by:

$$f_{nm} = \frac{c}{2\sqrt{\varepsilon_r}}\sqrt{\left(\frac{m}{a}\right)^2 + \left(\frac{2n+1}{2b}\right)^2} \quad c \quad \frac{1}{\sqrt{\mu_0\varepsilon_0}}$$

The lowest mode is TM_{00}.

$$f_{00} = \frac{c}{4b\sqrt{\varepsilon_r}} \quad o \quad b \quad \frac{\lambda_{00}}{\sqrt{\varepsilon_r}} \tag{13.4}$$

where

$$\lambda_{00} = \frac{c}{f_{00}} \tag{13.5}$$

This is to be compared with

$$b = \frac{\lambda_{01}}{2\sqrt{\varepsilon_r}}$$

where $\lambda_{01} = \frac{c}{f_{01}}$ for the rectangular patch.

Hence, to resonate at the same frequency, the length b for the shorted patch is half that of the regular patch. The shorted patch is known as t. quarter wave patch while the regular patch is known as the half-wave patch.

Using the cavity model, the various antenna characteristics of the shorted patch can be calculated following the procedures used for the regar patc'

3.2.1.3 *Experimental results*

Chair *et al.* [3] presented experimental results of the quarter-wave patch shown in Figure 13.3. The substrate between the patch and the ground plane is foam, with thickness h and relative permittivity 1.08. The sides of the patch are $a = b = 3.06\,\text{cm}$ long, with one side shorted. The patch is fed by a coaxial probe, with the feed point at $x = 0$, $y = d$, where d is the distance between the feed point and the open edge and is adjusted for best natch.

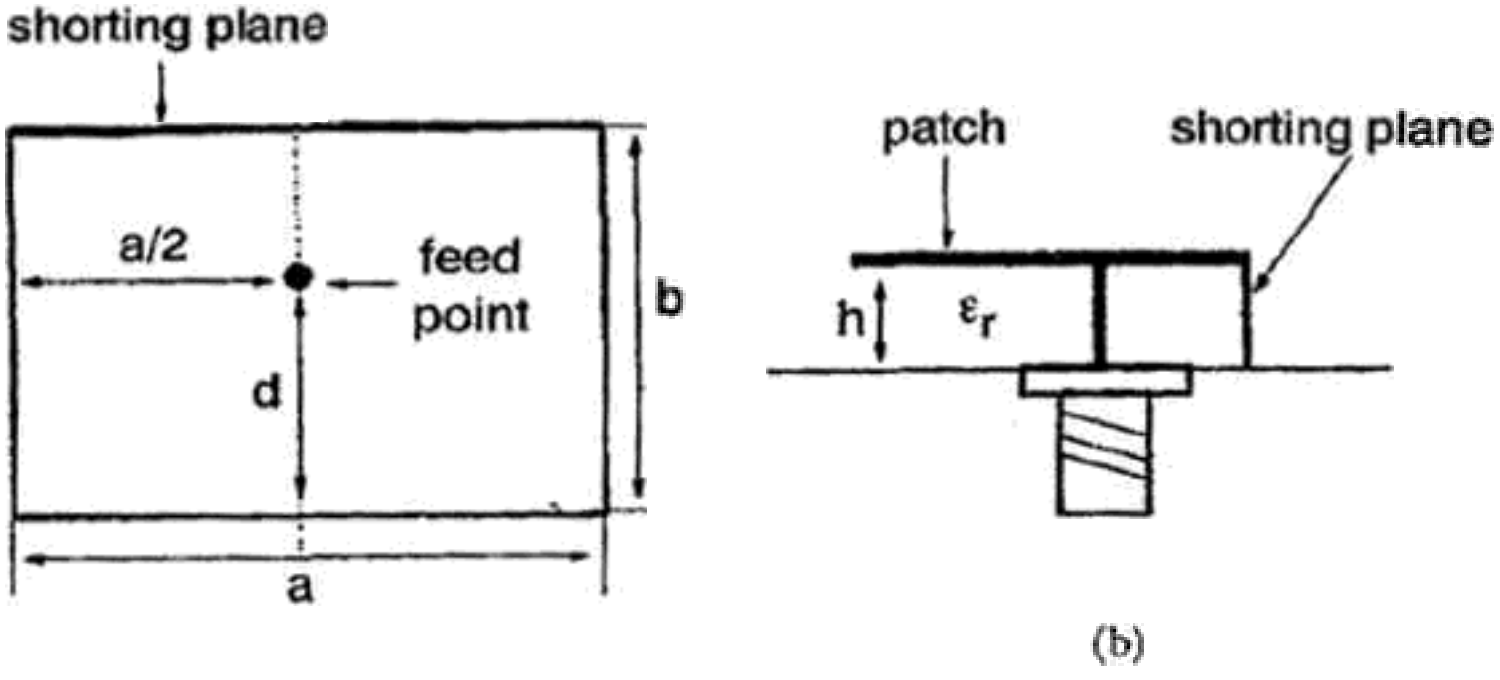

Fig. 13.3 Geometry of the shorted patch. (a) Top view; (b) Side view.

Table 13.1. Bandwidth Measurement (From [3] © 1999 John Wiley and Sons Inc., Reprinted with permission.)

		Quarter-wave patch			Half-wave patch		
C			BW (%)	Center Freq. (GHz)	d (mm)	BW	Center Freq.)
a	2	22	3.59	2.194	23	1.57	2.22
b	3	23	4.73	2.061	23	2.30	2.175
		20_	6.40	2.11	23	2.60	2.115
d	5	17	9.69	2.166	20	3.55	2.115
e	6	5	17.39	2.566	18	4.66	2.125
f	7	5	17.66	2.462	15	5.55	2.16

Pattern and bandwidth (VSWR = 2) measurements were performed for several thicknesses h. The results for bandwidth are summarized i Table 13.1.

It is noted in Table 13.1 that the shorted patch on foam substrate has relatively wide bandwidth. For $h = 7\,\text{mm}$, which corresponded to about $0.058\ \lambda_o$ at the center frequency, the impedance bandwidth was 18.54%. For comparison, for a half-wave regular patch of the same thickness and the same width but double in length, the measured impedance bandwidth, as shown in Table 13.1, was found to be only 5.55%. Comparisons with simulation results using Zeland IE3D software were in qualitative agreeme and are shown in Table 13.2(a) and 13.2(b). The shorter patch has a smaller volume and therefore less stored energy, leading to a smaller Q and large bandwidtl..

Table 13.2(a). Resonant frequencies and bandwidth of the shorted square patch of Figure 13.3 with $a = b = 3.06\,\text{cm}$ and $\varepsilon_r = 1.08$. (From [4] © 2000 IET. Reprinted with permission.)

		Experiment		Calculation	
h (mm)	d/b			f_o (GHz)	BW (%)
2	0.72	2.19	3.59	2.19	1.8
3	0.75	2.06	4.73	2.13	4.2
4	0.65	2.11	6.40	2.13	6.3
5	0.56	2.17	9.69	2.17	8.6
6	0.16	2.57	12.39	2.54	12.7
7	0.16	2.46	17.66	2.49	16.4

Table 13.2(b). Resonant frequencies and bandwidth of the regular rectangular patch of Figure 13.3 with $a = 3.06\,\text{cm}$, $b = 6.12\,\text{cm}$ and $\varepsilon_r = 1.08$. (From [4] © 2000 IET, Reprinted with permission.)

		Experiment		Calc_lation	
h (mm)	d/b	f_o (GHz)	BW (%)		%)
2	0.75	2.20	1.57	2.23	3.2
3	0.75	2.16	2.30	2.18	3.7
4	0.75	2.14	2.60	2.12	3.75
5	0.65	2.15	3.55	2.12	5.3
6	0.59	2.16	4.66	2.13	6.3
7	0.49	2.20	5.55	2.16	7.3

The measured E and H plane patterns at the center frequency for each of the six cases in Table 13.1 are shown in Figures 13.4 (a)–(f). The measurements were made with the feed positions indicated.

The measured patterns showed large cross polarization in the E-plan They also showed that, depending on the thickness, the maximum radiation could occur off broadside. The measured gains as a function of frequency in the broadside direction as well as in the maximum direction are shown in Figures 13.5(a)–(c) for $h = 3, 5$, and 7 mm. The gain values [4] at the sonant frequencies are summarized in Table 13.3. It is seen that typical values of the maximum gain were in the range 2–3.5 dBi. This is about half at of the regular half-wave patch

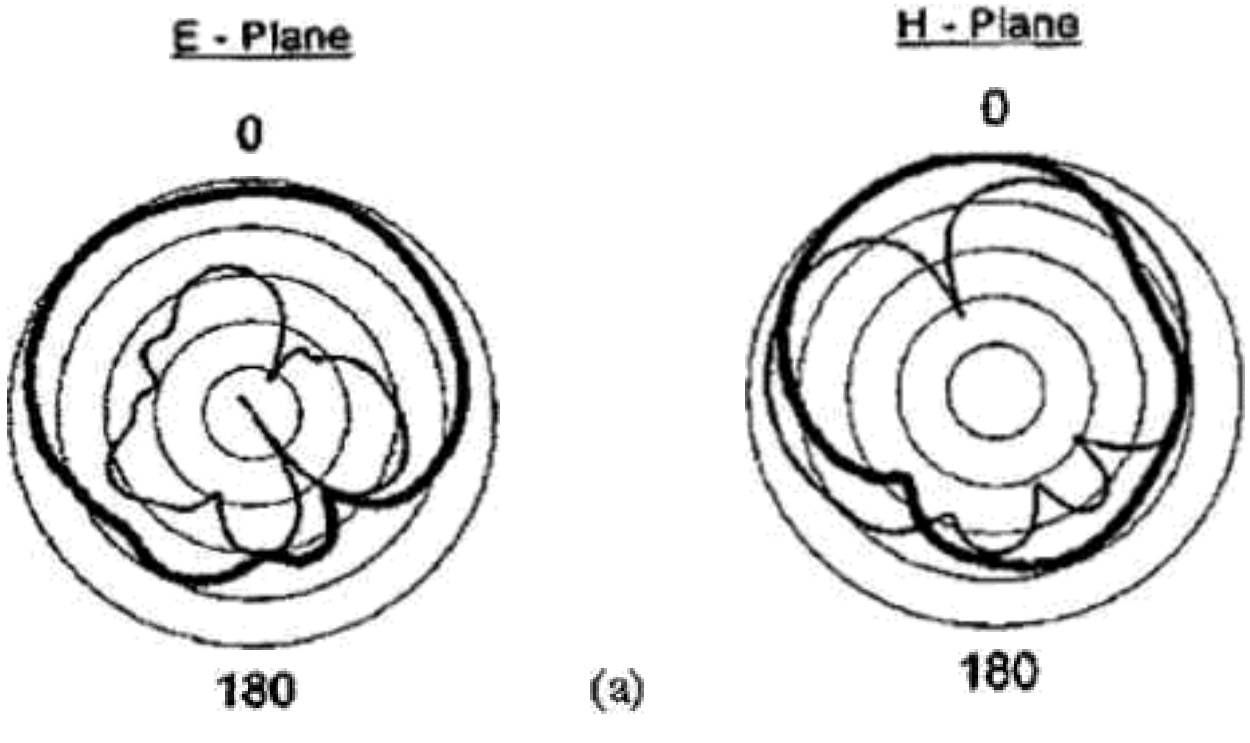

Fig. 13.4 Copolarization and cross-polarization patterns at the center frequencies for the six cases shown in Table 13.1. Co-pol, –x-pol. 10 dB/div. (From [3] © 999 John Wiley and Sons Inc., Reprinted with permission.)

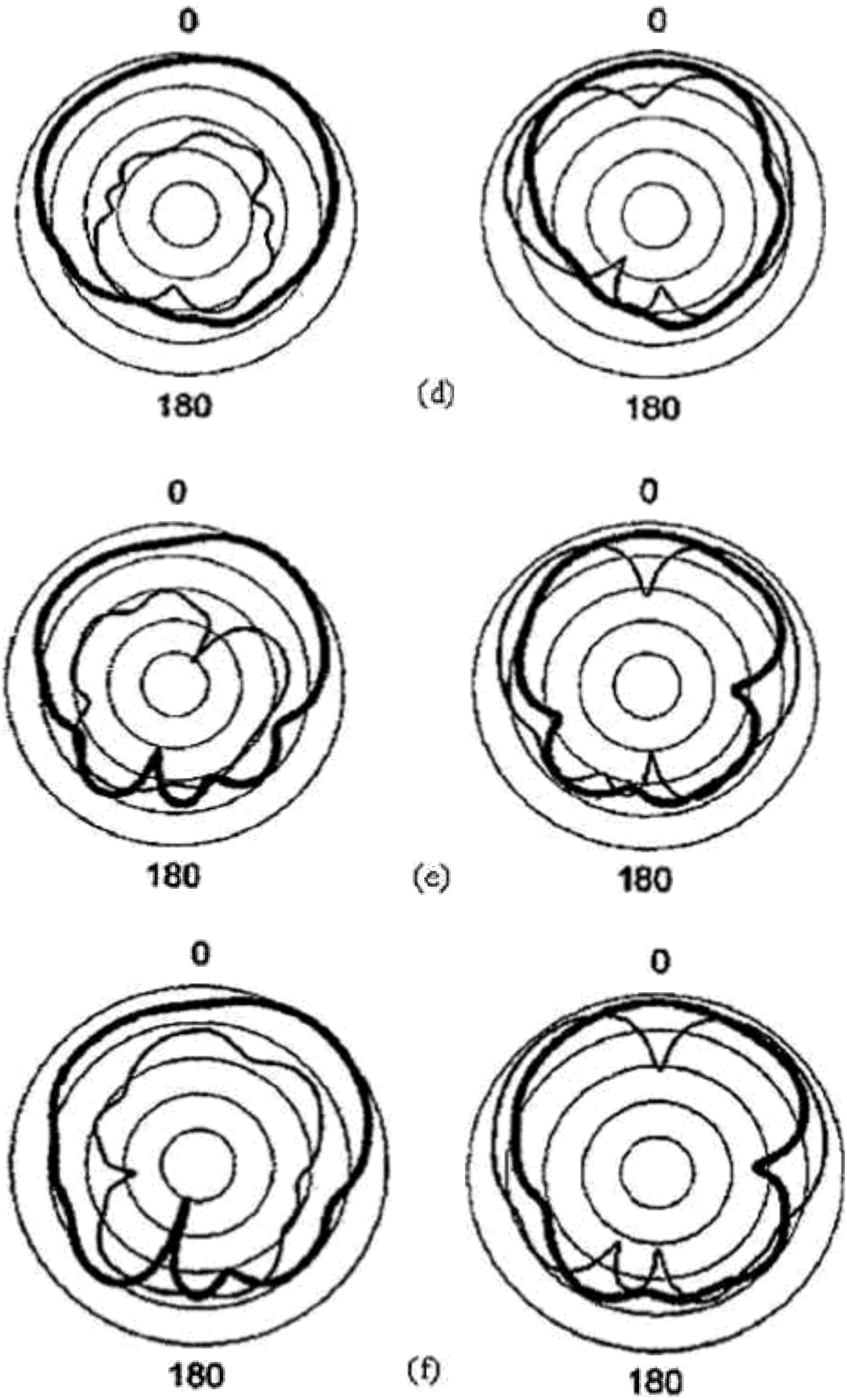

Fig. 13.4 (*Continued*)

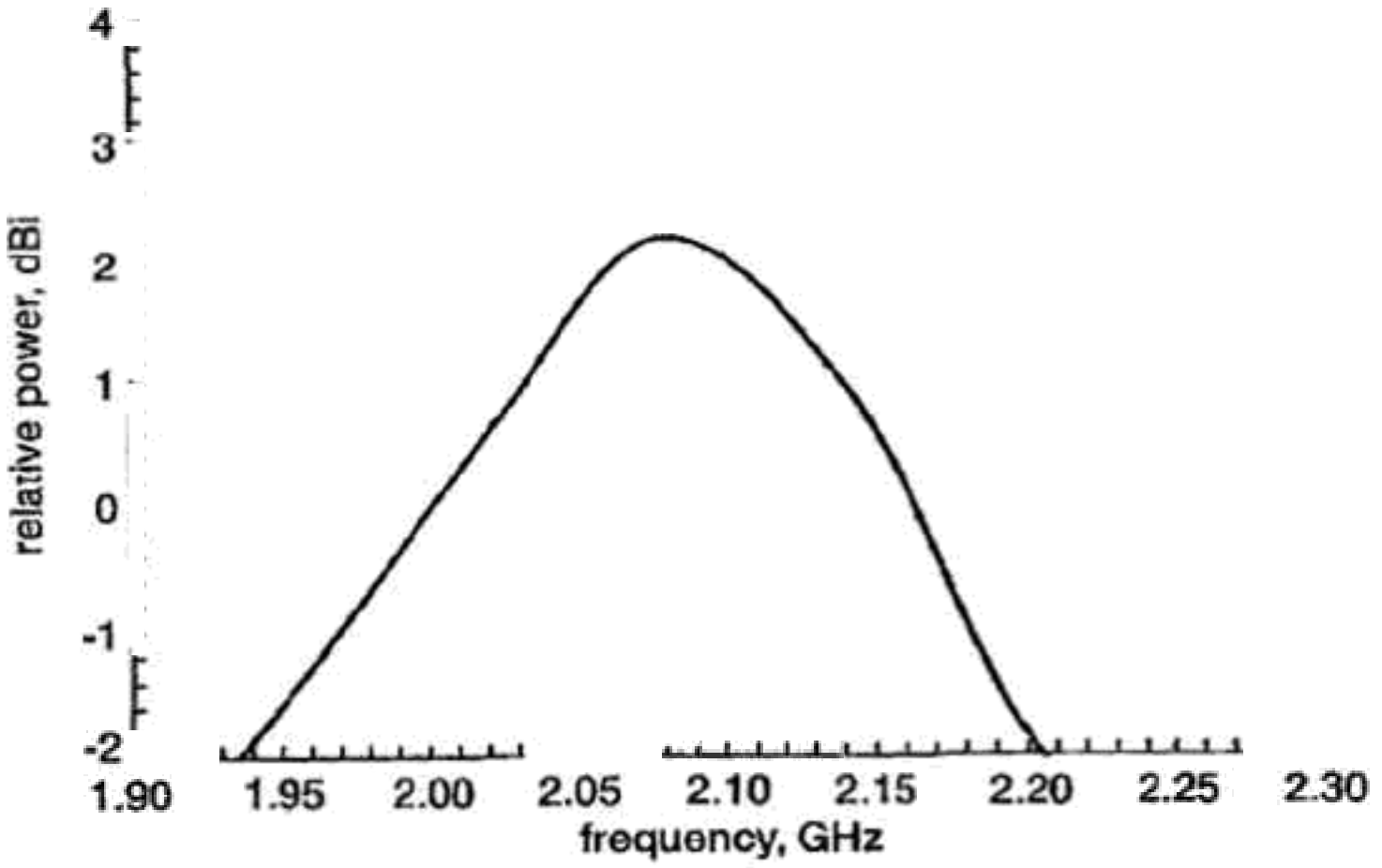

(a)

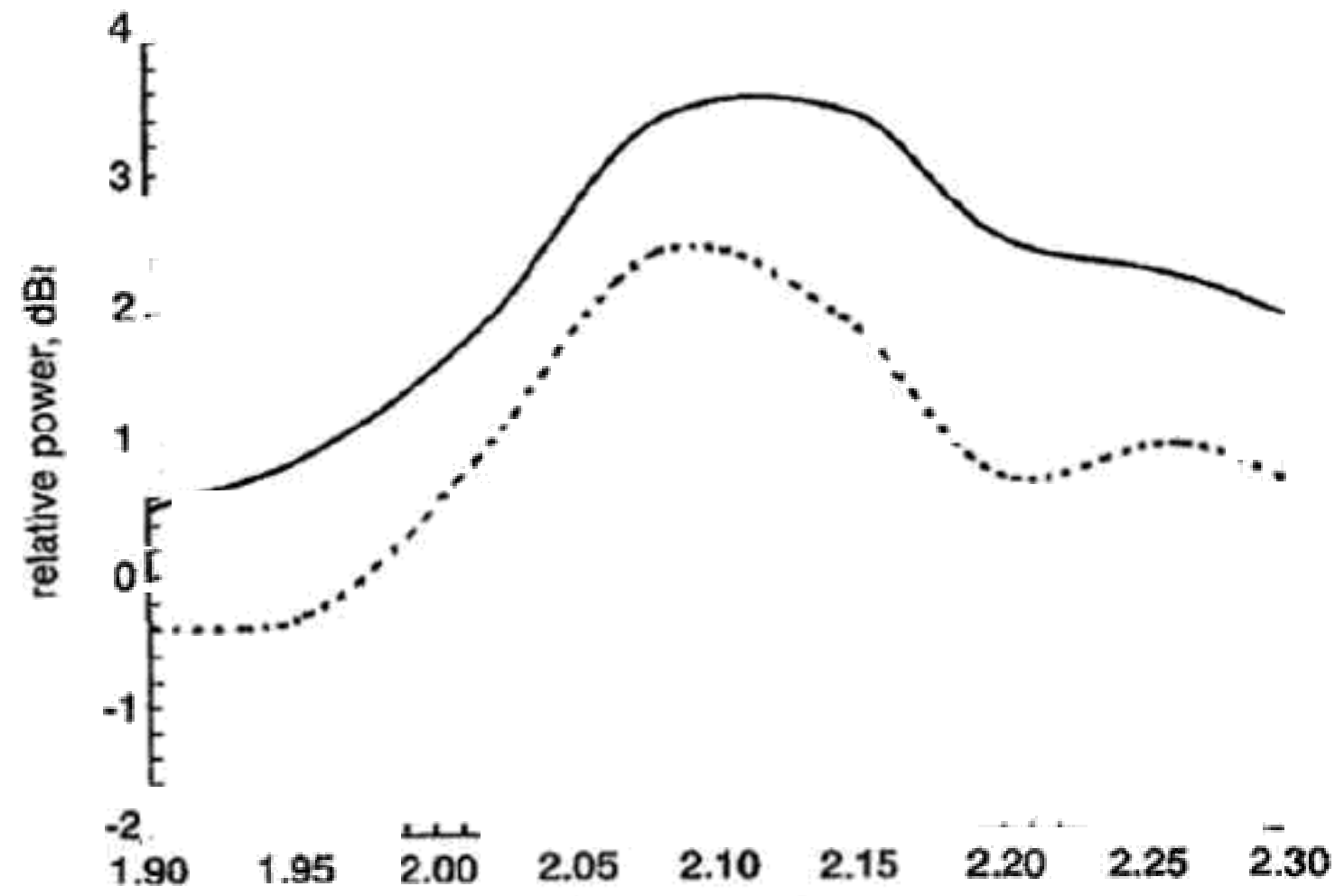

(b)

Fig. 13.5 Measured gains at maximum direction and at broadside for patch of Figure 13.3. (a) $h = 3\,\text{mm}$, maximum direction is in broadside, (a) $h = 5\,\text{mm}$, maximum direction is at 30°, (a) $h = 7\,\text{mm}$, maximum direction is at 45°, ____ Maximum direction, —— broadside, (From [4] © 2000 IET, Reprinted with permission.)

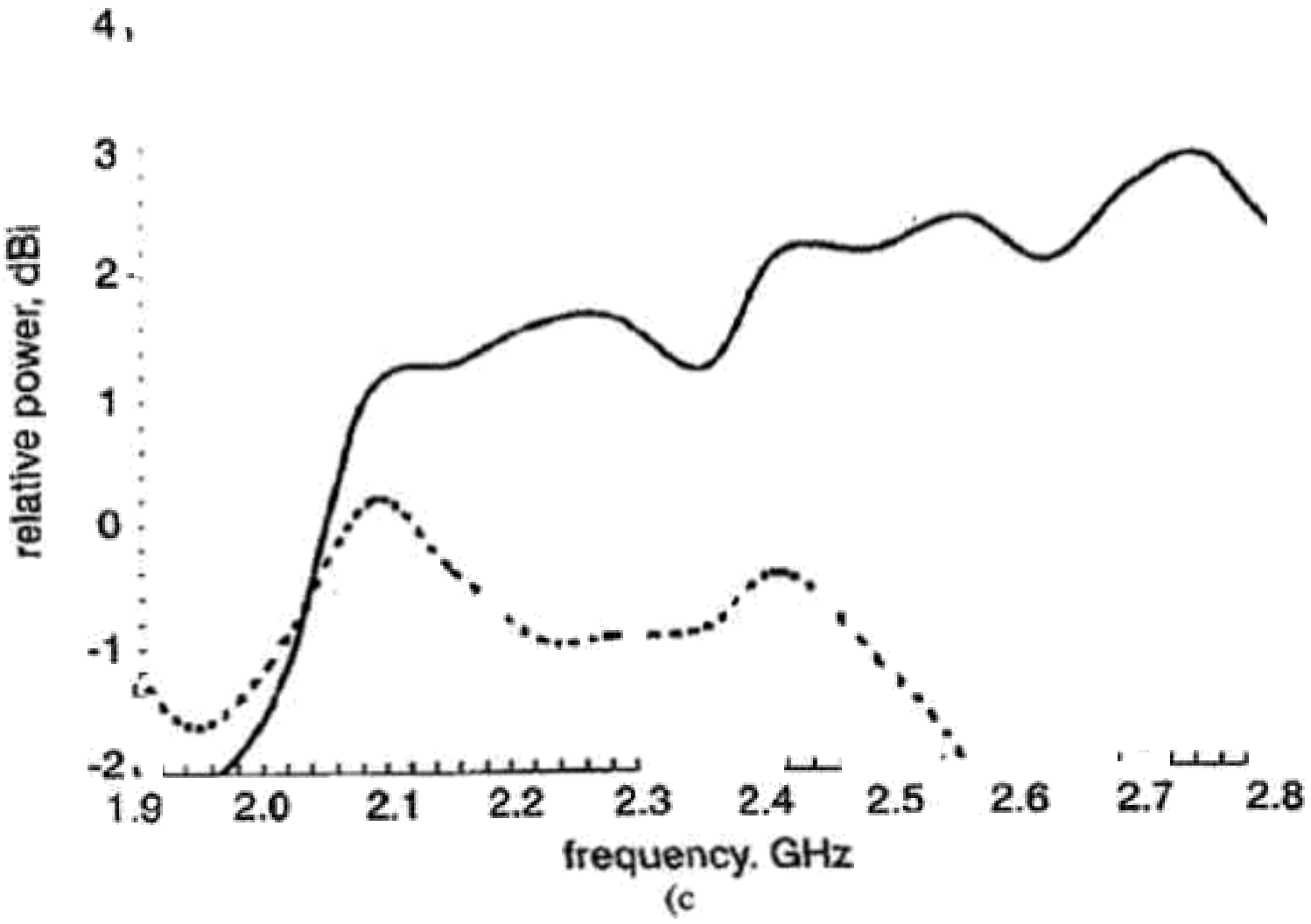

Fig. 13.5 (*Continued*)

Table 13.3. Measured gain of ıe shorted square patch of ⁻gure 13.3. (From [4] © 2000 IET, Reprinted with permission.)

h (mm)	f_o (GHz)	Gain (dBi) broadside	Maximum direction $\theta°$
3	2.06	2.5	2.5 at 0°
5	2.17	2.5	3.5 at 30°
7	2.46	0.2	2.2 at 45°

$\theta°$ is measured from the perpendicular direction in the E-plane (perpendicular to the shorting plane).

13.2.2 *Partially Shorted Patch and Planar Inverted ⁻' Antenna*

Figure 13.6 shows the geometry in which the shorting wall, instead of extending fully across the width of the patch a, has a width s, where $s \leq a$.

It was shown in Hirasawa and Haneishi [5] that the use of a partially shorted wall had the effect of reducing the resonant frequency of the antenna. Lee *et al.* [4] showed that this was accomplished at the expense of bandwidth. Their calculated results using Zeland IE3D simulation software

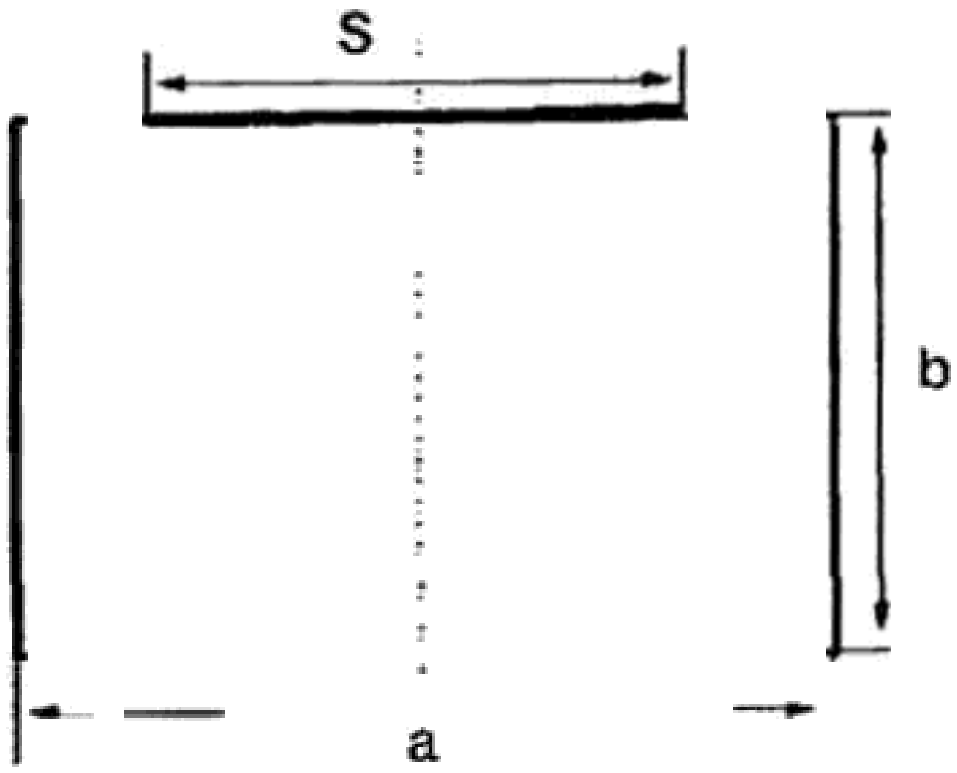

Fi.. 3.6 Geometry of partially shorted patch.

were shown in Figure 13.7 for an antenna with $a = 3.8\,\text{cm}$, $b = 2.5\,\text{cm}$, $h = 3.2\,\text{cm}$ and $\varepsilon_r = 1.0$. It is seen that, as s/a decreased from 1.0 to 0.1, ·he resonant frequency decreased from 2.69 to 1.61 GHz, representing a 60% eduction in frequency or size. However, the bandwidth. was reduced from 7.4% for $s/a = 1.0$ to 3.7% for $s/a = 0.1$

he partially shorted patch in the form shown in Figure 13.8 is known as the planar inverted F antenna (PIFA), because the side view looks like an inverted F. The width of the shorting wall w is approximately $0.2\,L_1$ while the dimensions of L_1 and L_2 are on the order of $1/8\lambda_o$.

13.2.3 *Use of Shorting Pin*

-nother technique for reducing the patch size, very similar to the inverted-F method, is to use a shorting pin [6]. This is illustrated in Figure 13.9.

The shorting pin causes the fields underneath the patch to bounce back-and-forth. The field starts to radiate once the bouncing distance reaches half-wavelength. As a result of the multiple bounces, the physical size of :he patch is reduced. Since the bounces are non-unidirectional, the fields can radiate out from almost all edges of the patch, resulting in high cross-polarization. However, for certain applications such as cellular phone communication in a multi-path environment, high cross-polarized fields are not ·oncern.

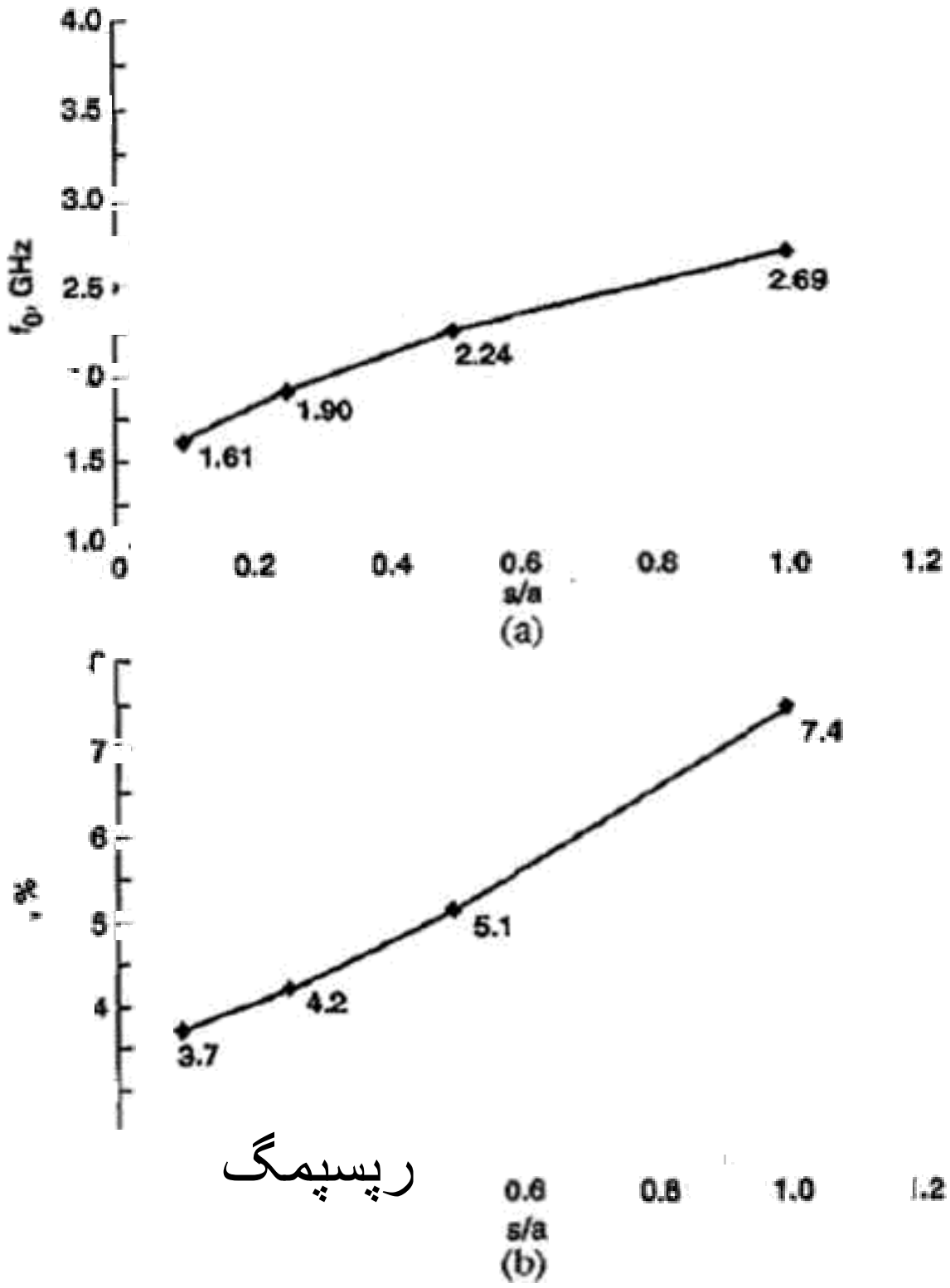

Fig. 13.7 Calculated resonant frequency and bandwidth of partially shorted with $= 3.8\,\text{cm}$, $b = 2.5\,\text{cm}$ on foam substrate ($\varepsilon_r = 1$) of thickness $h = 3.2\,\text{mm}$. (a) Resonant frequency and (b) Bandwidth. (From [4] © 2000 IET, Reprinted with permission.)

If the shorting pin is close to the feed, the resonant circuit of the patch is capacitively coupled to the pin. This is equivalent to increasing the permittivity of the substrate, which further contributes to reduction in frequency or size of the patch (measured in wavelength).

Figure 13.10 shows a circular patch with one shorting pin on foam substrate. Using Zeland IE3D simulation software, for the dimensions given in the figure, the results for the return loss are given by the solid curve of Figure 13.11. The radius of the patch is reduced by a factor of 3 and the

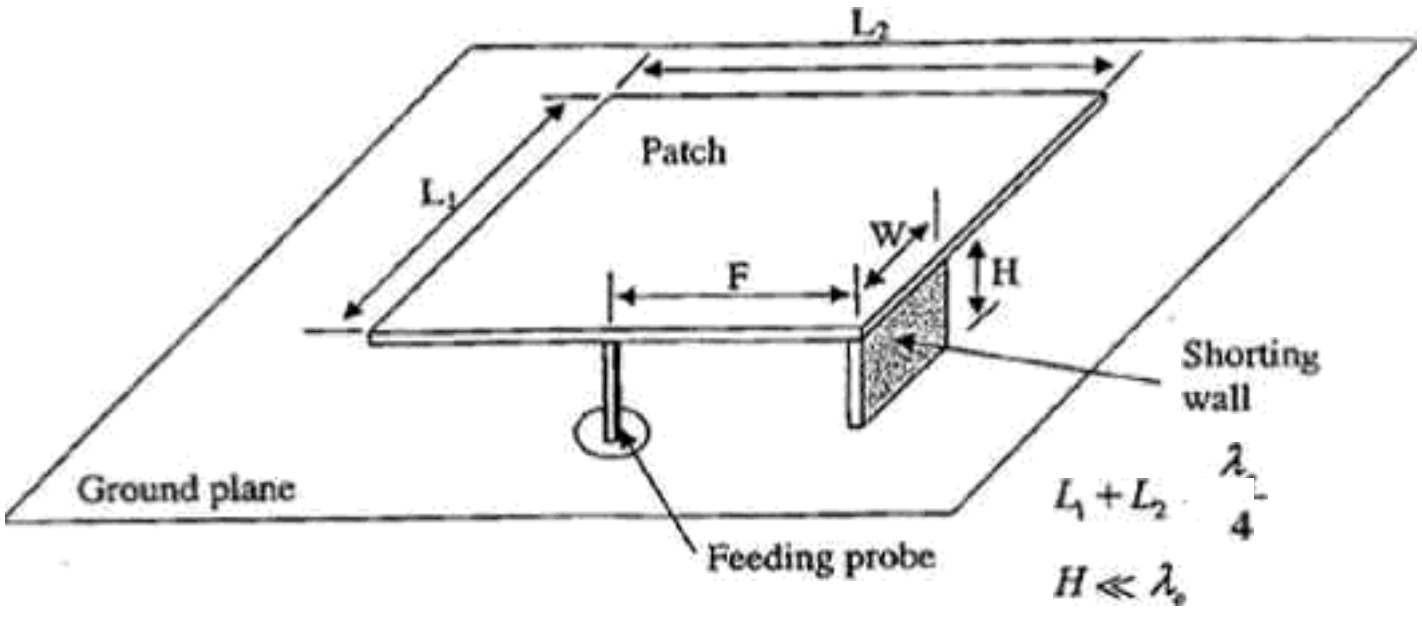

Fig. 13.8 Size reduction by using an inverted-F patch.

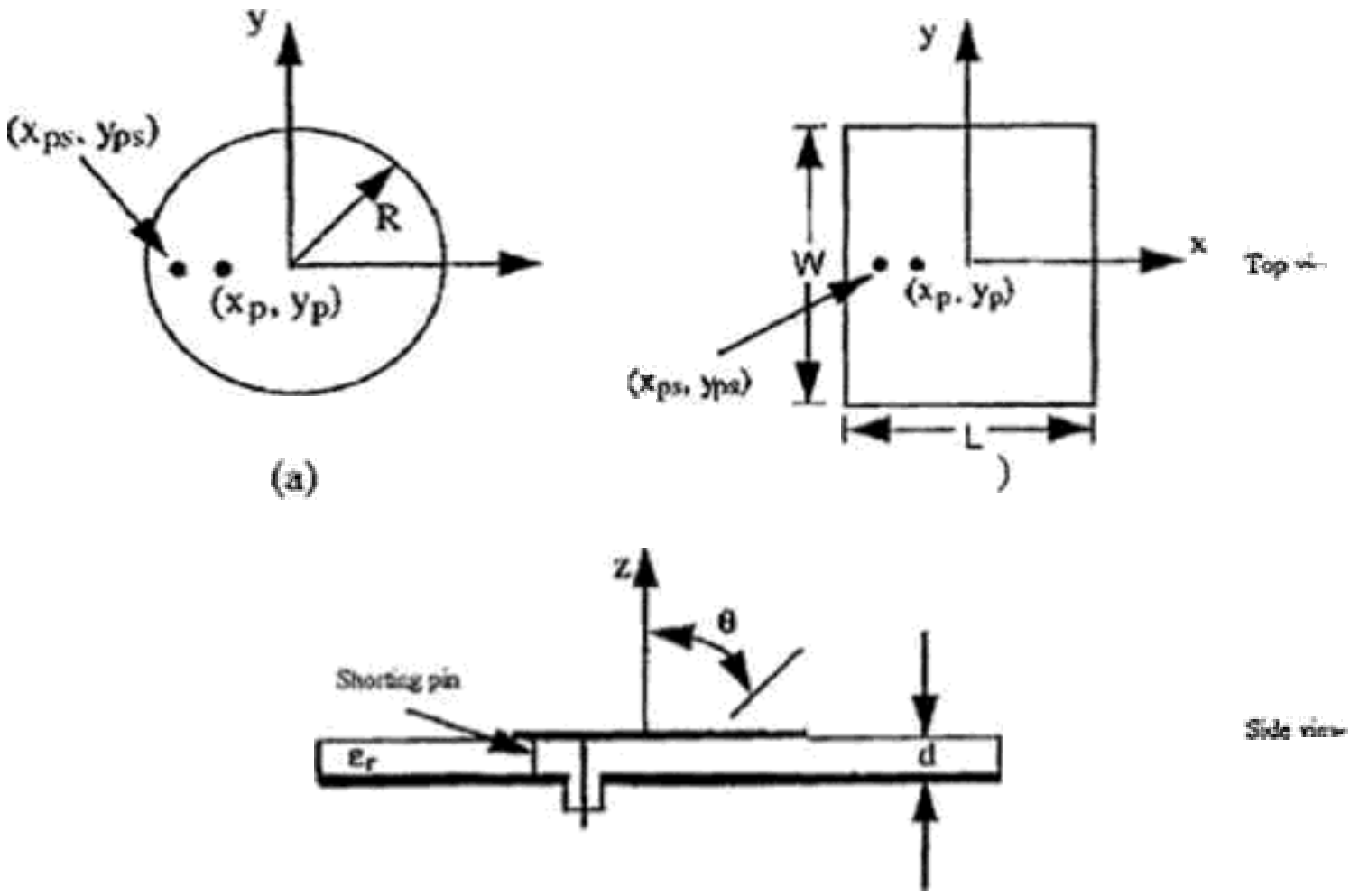

Fig. 13.9 Circular (a) and rectangular (b) patches with shorting post.

area by a factor of 9 when compared to the case of no shorting pin. The thickness of the foam substrate is $0.06\lambda_o$, and the impedance bandwidth is about 6.3%. The simulated radiation patterns at 1.9 GHz are shown in Figure 13.12. As noted earlier, the cross polarization of this type of antenna is very high. The simulation results are consistent with the experiments reported in [6].

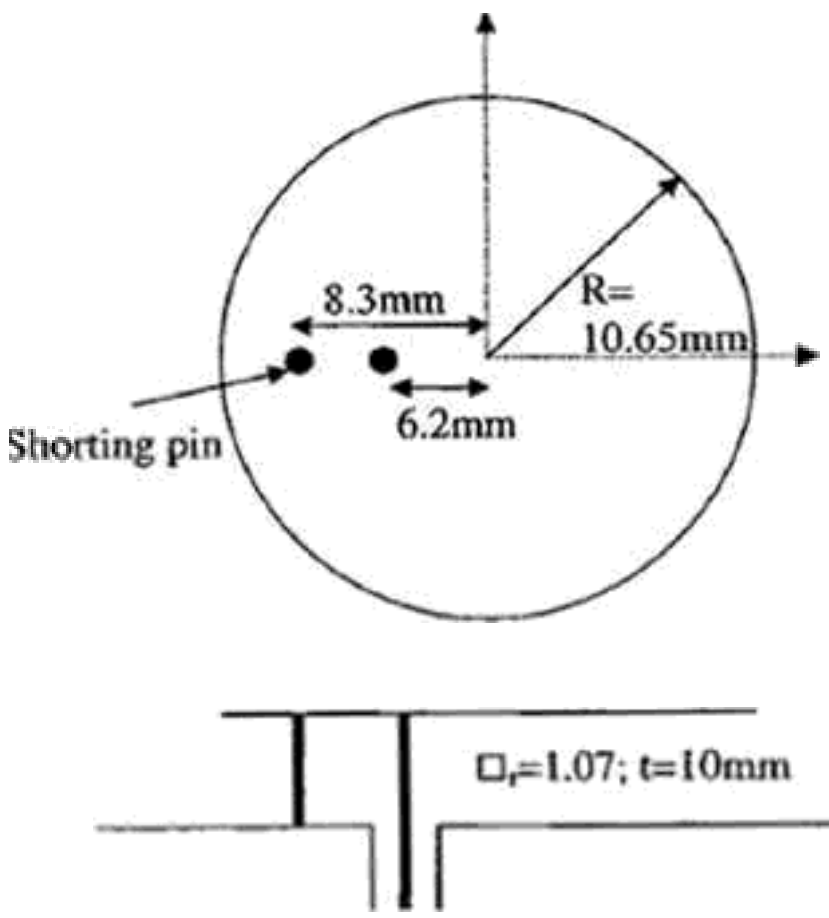

ig. 13.10 Geometry of the circular patch antenna with shorting pin (not to scale).

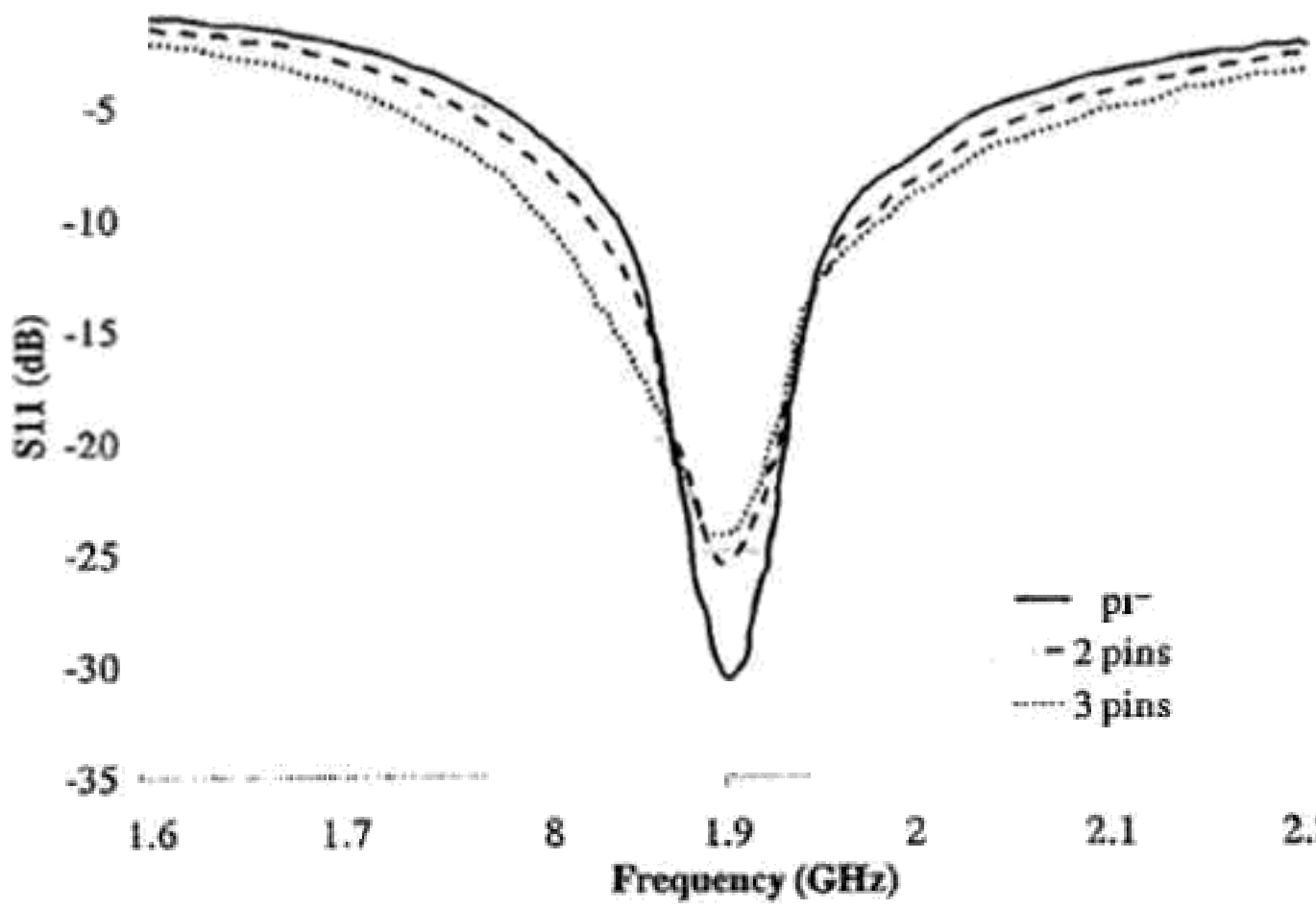

Fig. 13.11 Simulated return loss of the miniature patch antenna with different number of shorting pin...

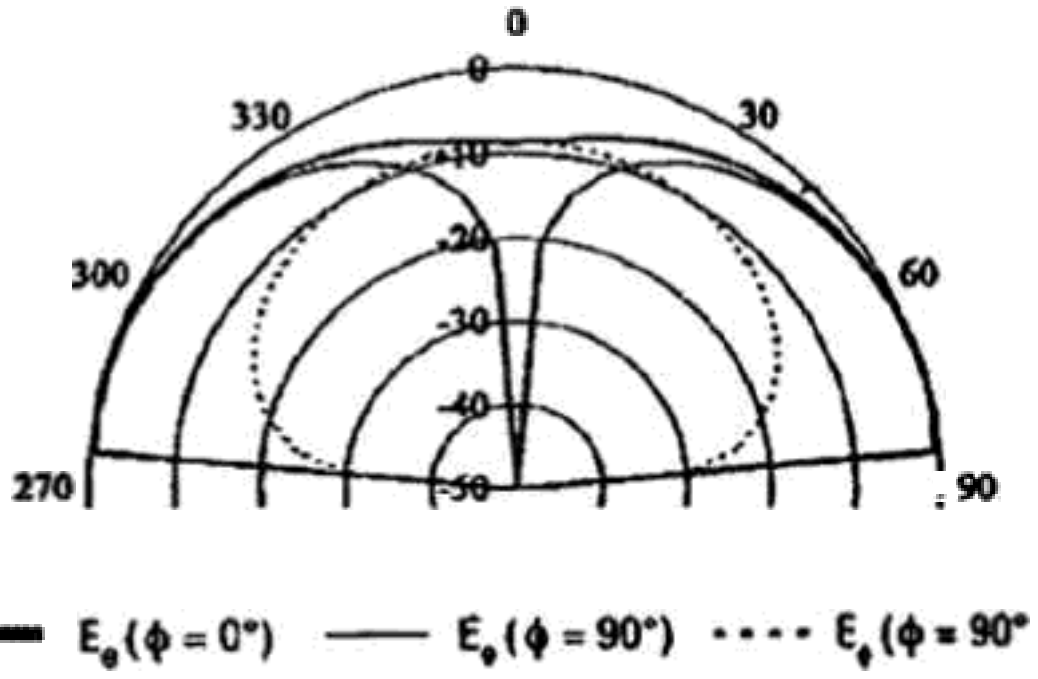

Fig. 13.12 Simulated radiation pattern of the miniature patch antenna with 1 shorting pin at 1.9 GHz (10 dB/div`

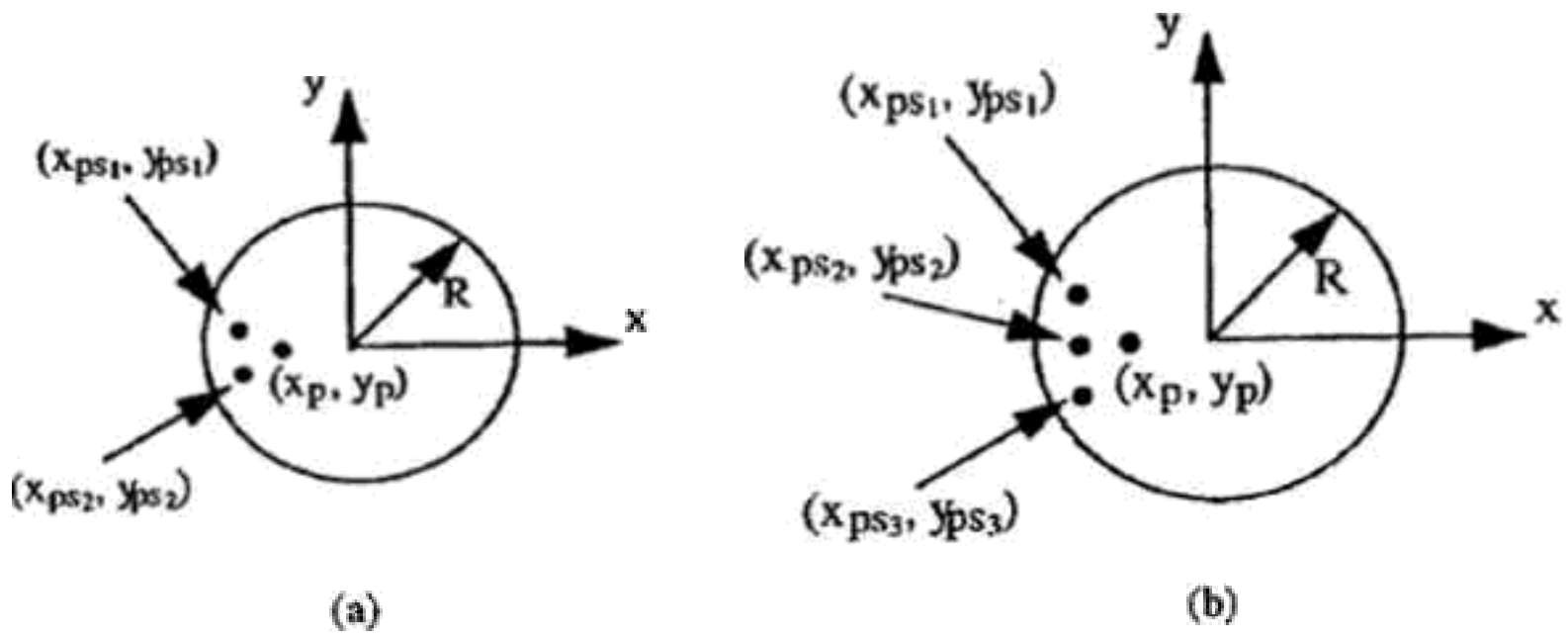

"g. 13.13 Circular patch with (a) 2 and (b) 3 shorting pins (units in mm and not to scale). (a) $R = 13.2$, $x_p = 4.95$, $x_{ps1} = x_{ps2} = 11.08$, $y_{ps1} = 1.95$, $y_{ps2} = -1.95$, (b) $R = 15.4$, $x_p = 2.35$, $x_{ps1} = 13.3$, $x_{ps2} = x_{ps3} = 14.1$, $y_{ps1} = 0$, $y_{ps2} = 5.13$, $y_{ps3} = -5.13$.

The bandwidth can be improved by using multiple shorting pins [6]. A circular patch with two and three shorting pins are shown in Figures 13.13(a) and Figure 13.13(b). The simulated return loss for these cases are shown in the broken curves of Figure 13.11. The impedance widths are 7.9% for the patch with 2 pins and 10.0% for t' e patch with 3 pins.

13.2.4 *The Folded Pat*

Both the shorting wall and shorting pin size reduction techniques result in high cross polarization levels. A method which maintains a relatively low

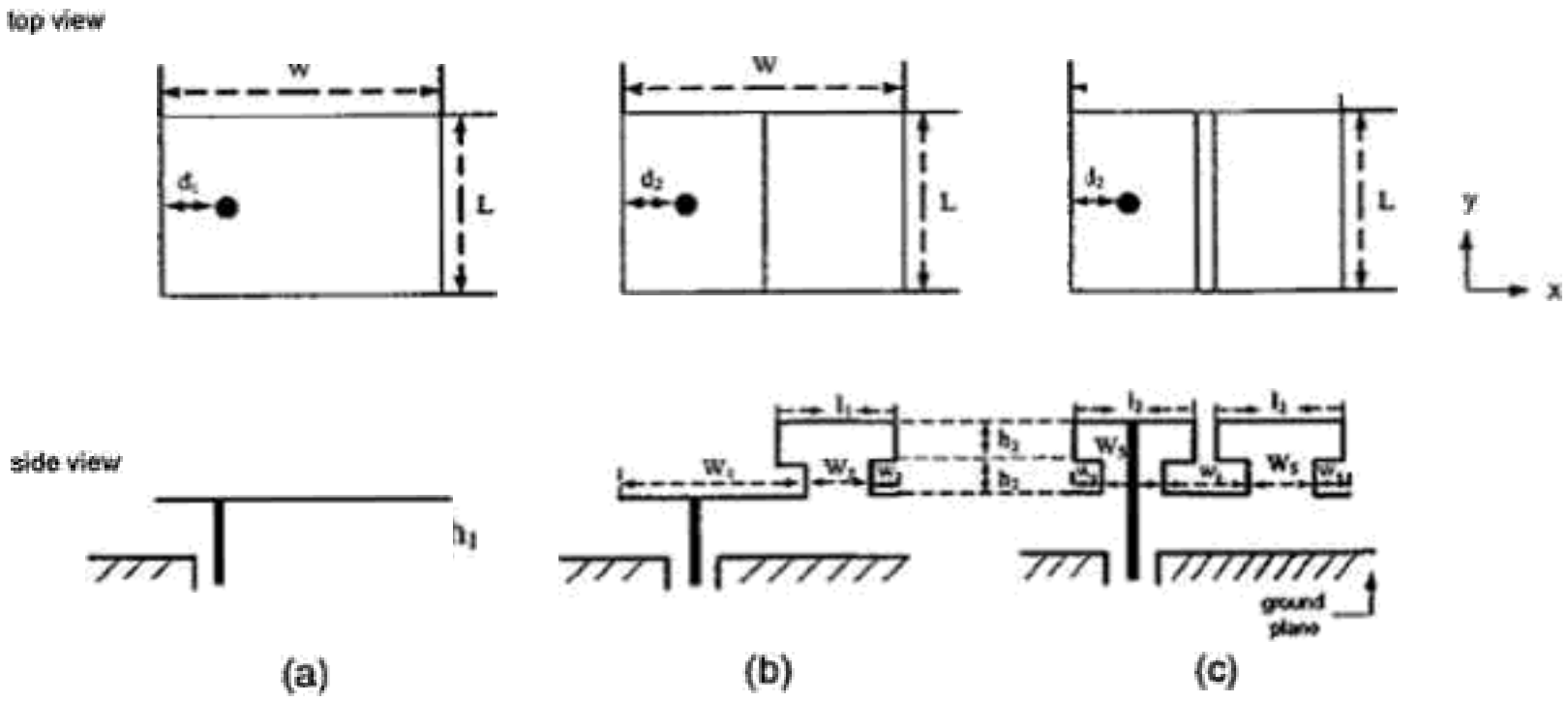

Fig. 13.14 Structures of patches and antenna. $W = 31\,\text{mm}$, $L = 51\,\text{mm}$, $d_1 = 20\,\text{mm}$, $d_2 = 15\,\text{mm}$, $h_1 = 2\,\text{mm}$, $h_2 = 3\,\text{mm}$, $w_1 = 9.5\,\text{mm}$, $w_2 = 5\,\text{mm}$, $l_1 = 10\,\text{mm}$, $l_2 = 15\,\text{mm}$, $l_3 = 15\,\text{mm}$, $l_4 = 23\,\text{mm}$. (From [8] © 1999 IET, Reprinted with permission.)

cross polarization level is that of the folded patch, first introduced by Chair *et al.* [7–10].

Consider the geometries shown in Figure 13.14.

Figure 13.14(a) presents a conventional patch antenna with length $L = 51\,\text{mm}$ and $W = 31\,\text{mm}$. The antenna excited in the TM_{01} mode is used as a reference. Figure 13.14(b) shows a folded patch antenna, designated as folded-patch configuration 1, which is made of a copper sheet of length 85.5 mm and width 31 mm. Figure 13.14(c) shows a second folded patch antenna designated as folded patch configuration 2, which is made of a copper sheet of length 111 mm and width 31 mm. The antennas are fed by coaxial probes. Although all three antennas have the same length in the top view, it is found that the resonant lengths of the folded patches are effectively longer than the length of the conventiona pat

The measured SWR versus frequency of the three antennas are shown in Figure 13.15.

he resonant frequency for the conventional patch is 2.65 GHz. Folded-patch configuration 1 had a resonant frequency of 2.1 GHz (20.75% decrease) while that of folded-patch configuration 2 was 1.66 GHz (37.26% decrease). The gains of the two configurations were 6.1 and 5.8 dBi, respectively (Figure 13.16) and were larger than the quarter wave shorted patch.

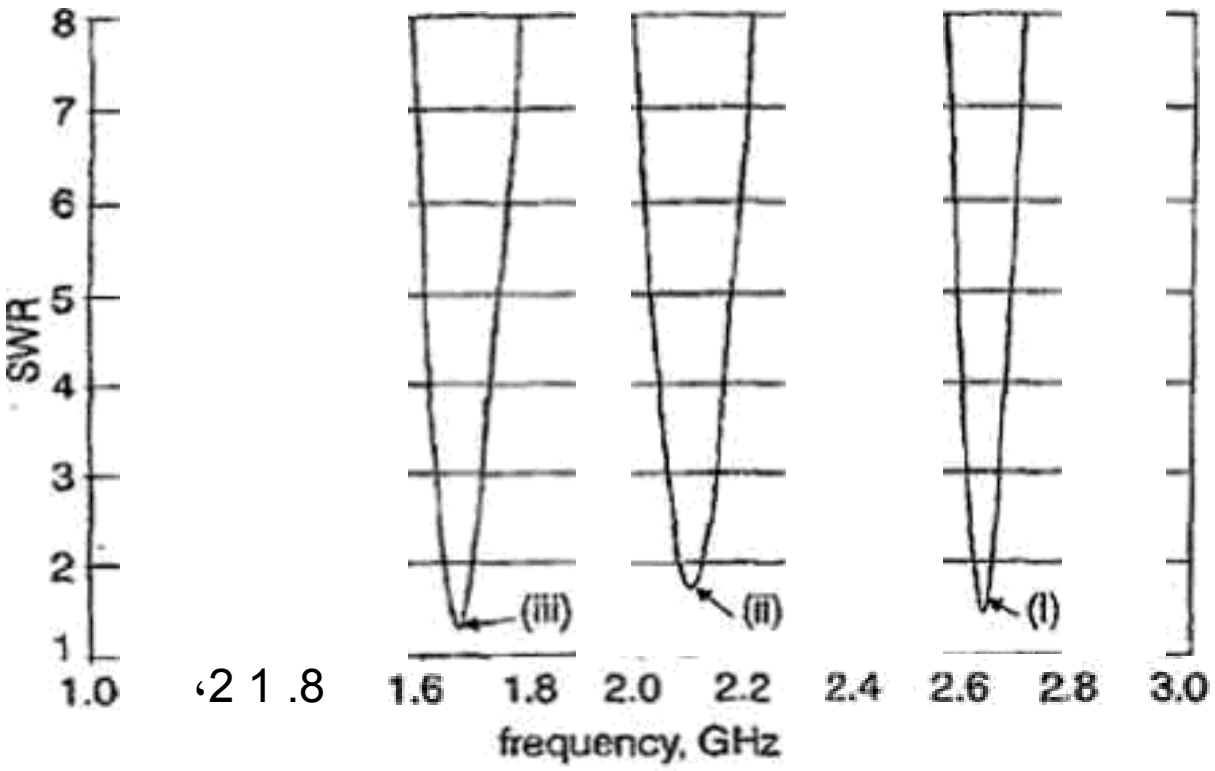

Fig. 13.15 SWR against frequency. (i) single layer patch: $f_o = 2.65\,\text{GHz}$, BW = 1.23% (ii) folded-patch configuration 1: $f_o = 2.1\,\text{GHz}$, BW = 2.03% (iii) folded-patch configuration 2: $f_o = 1.66\,\text{GHz}$, BW = 3.16% (From [8] © 1999 IET, Reprinted with permission.)

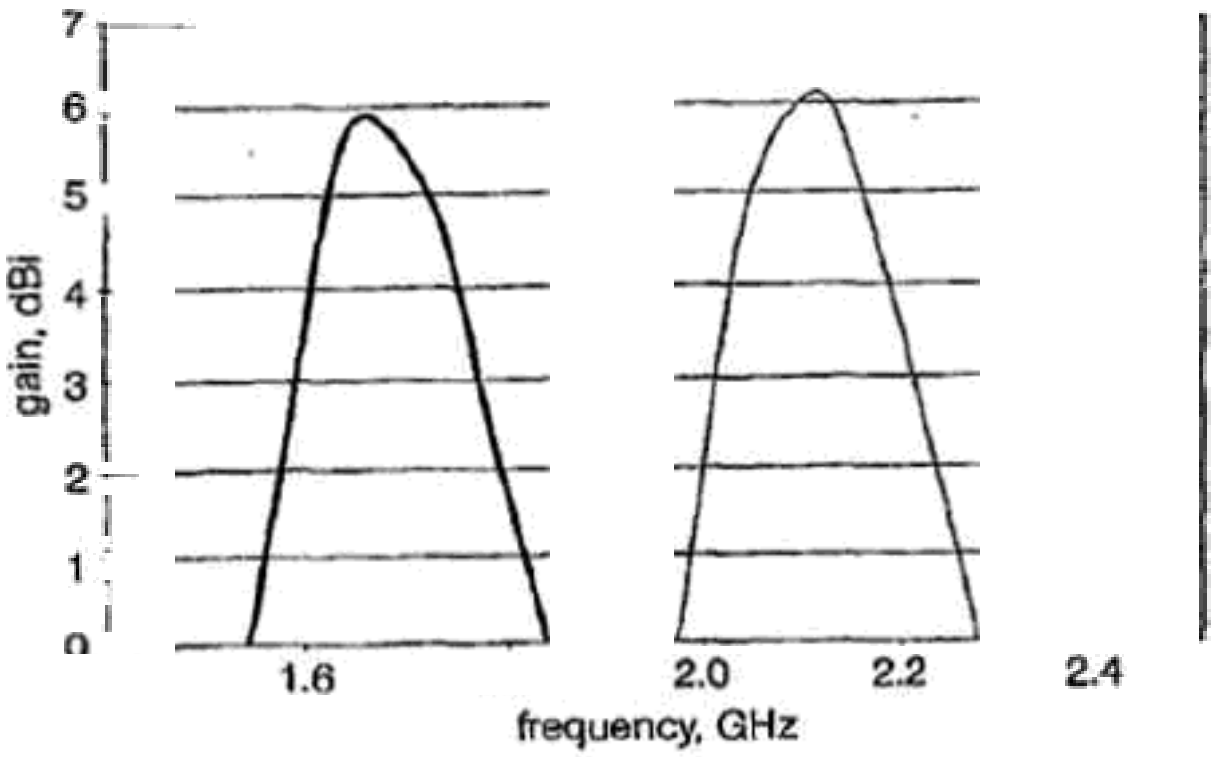

Fig. 13.16 Measured gain. —- Configuration 1, ___ Configuration 2 (From [© 1999 IET, Reprinted with permission.)

The radiation patterns of the folded patch configurations were measured at 2.1 and 1.66 GHz, respectively, and are shown in Figures 13.17 and 13.1[illegible]. The co-polarization patterns had maxima in the broadside direction. The cross polarization maximum was −20 dB below the co-polarization maximum. This was significantly lower than that of a shorted quarter-wave patch or patch with shorting pin.

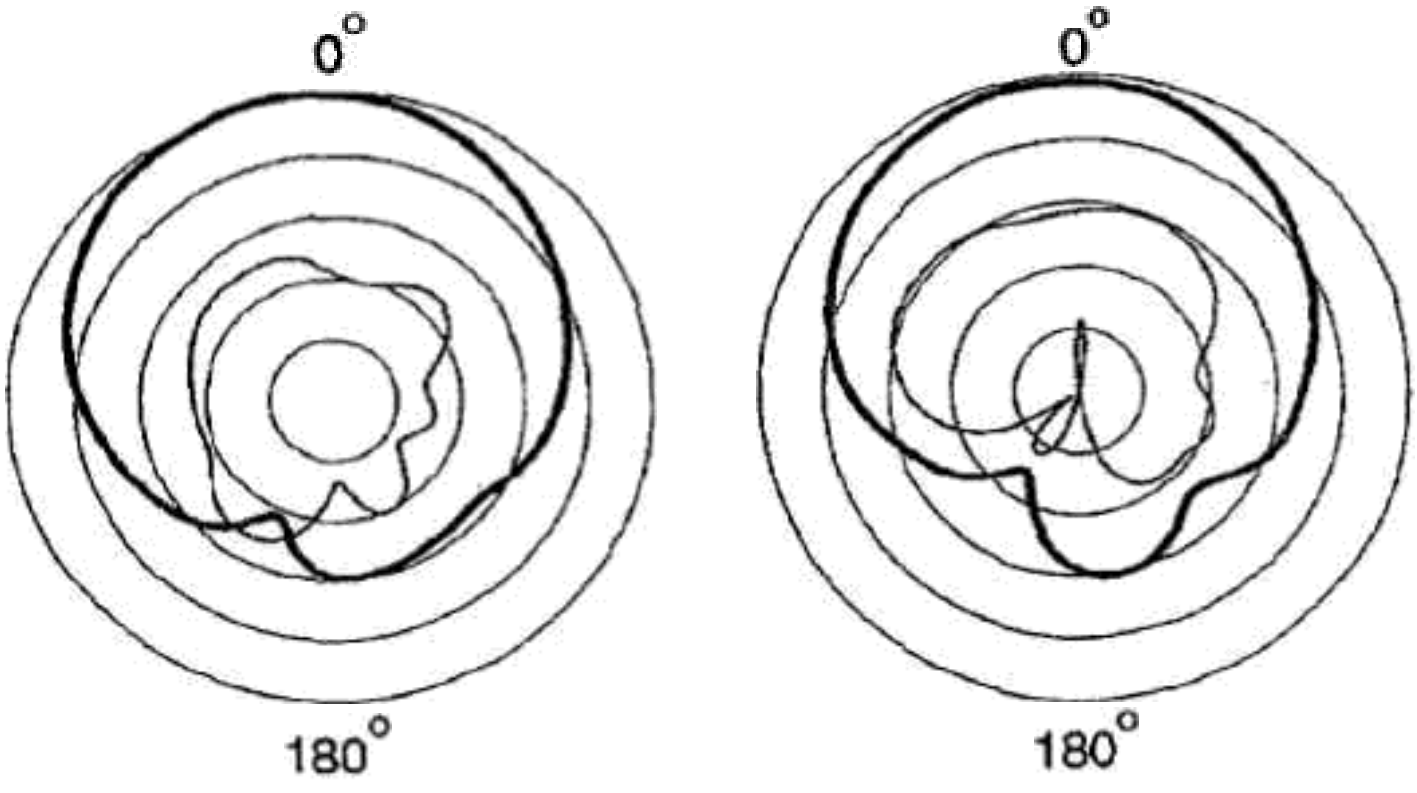

Fig. 13.17 Folded-patch configuration 1 radiation pattern. (a) E-plane, (b) H-plane, — Co-polarization, ___ Cross-polarization, 10 dB/div (From [8] © 1999 IET, Reprinted with permission.)

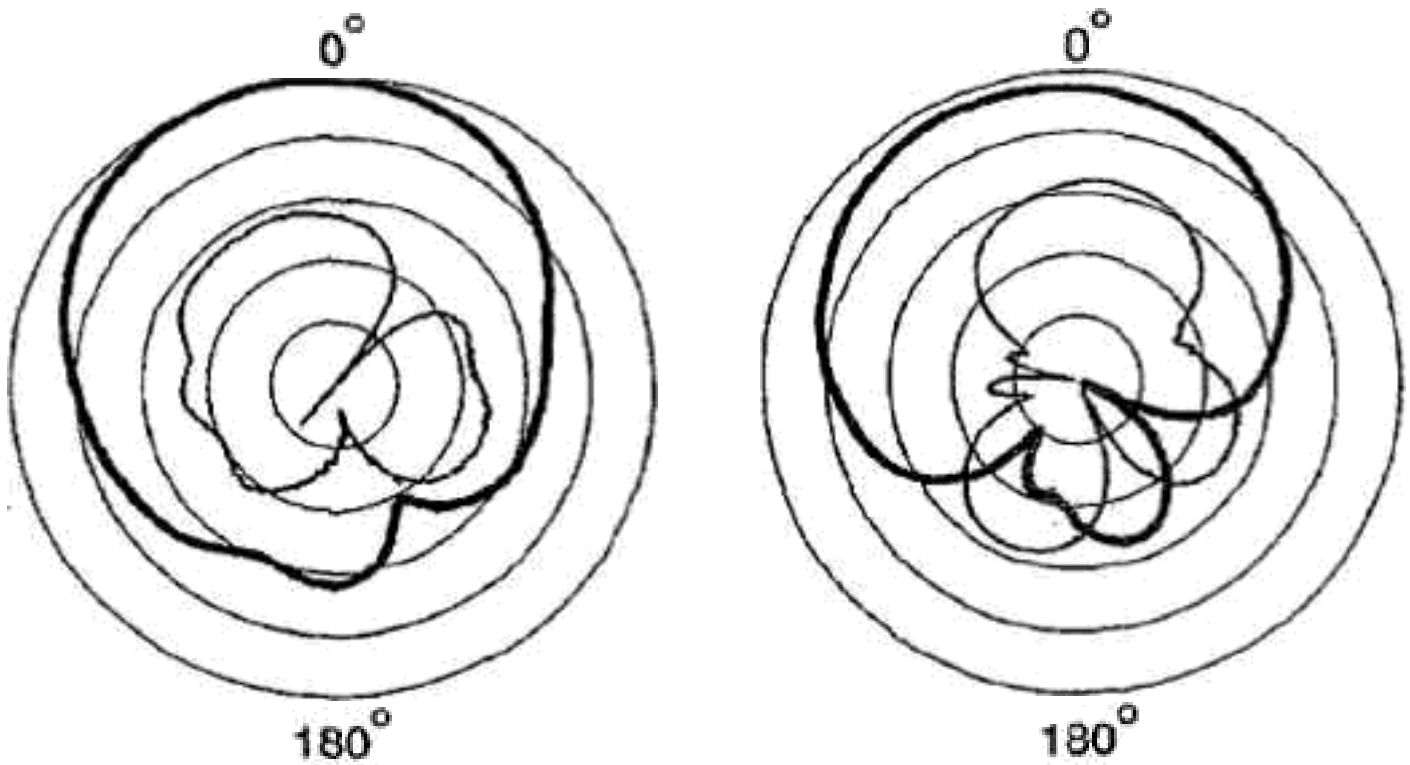

ig. 13.18 Folded-patch configuration 2 radiation pattern. (a) E-plane, (b) H-plane, — Co-polarization, ___ Cross-polarization, 10 dB/div (From [8] © 1999 IET, Reprinted with permission.)

.3.3 Small-Size Wide-Bandwidth Patch Antennas

he broadbanding techniques discussed in chapters 9 and 11 can be combined with the size reduction techniques to obtain small-size patch antennas exceeding 20% impedance bandwidth, These are the topics of this section,

which are based mainly on the simulation results summarized in the review paper by Shackelford *et al.* [11]. Experimental results supporting the conclusions can be found in that reference and the references cited therein [12, 13]

13.3.1 *The U-Slot Technique*

13.3.1.1 *U-slot patch antenna on high dielectric constant substrates*

Wideband U-slot antennas (Figure 13.19) are usually designed on foam or air substrates, resulting in patches with a resonant length of about $0.5\lambda_o$.

To decrease the resonant length, simulation results of these patch antennas on substrates with several values of the dielectric constant are shown in Table 13.4. These results were obtained using the Ansoft Ensemble sof ware. The patch dimensions, thickness, normalized area, and bandwidth are shown in Table 13.4a. As the dielectric constant of the substrate material was increased from 1.0 to 4.0, the area of the patch was decreased by 77% and the bandwidth was decreased from 42% to 22%, still a substantial bandwidth. The substrate thickness decreased from $0.8\lambda_o$ to $0.7\lambda_o$. The simula tion results also shown that this trend continued when ε_r was increased to 9.8. However, this will reduce the radiation efficiency due to surface waves. The design parameters for these antennas are shown in Table. 13.4b.

3.3.1.2 *U-slot patch antenna with shorting wall*

To further reduce the size of the U-slot patch antenna, a shorting wall is introduced, as shown in Figure 13.20. Table 13.5(a) shows the simulation results obtained for several values of ε_r, designed at a center frequency of

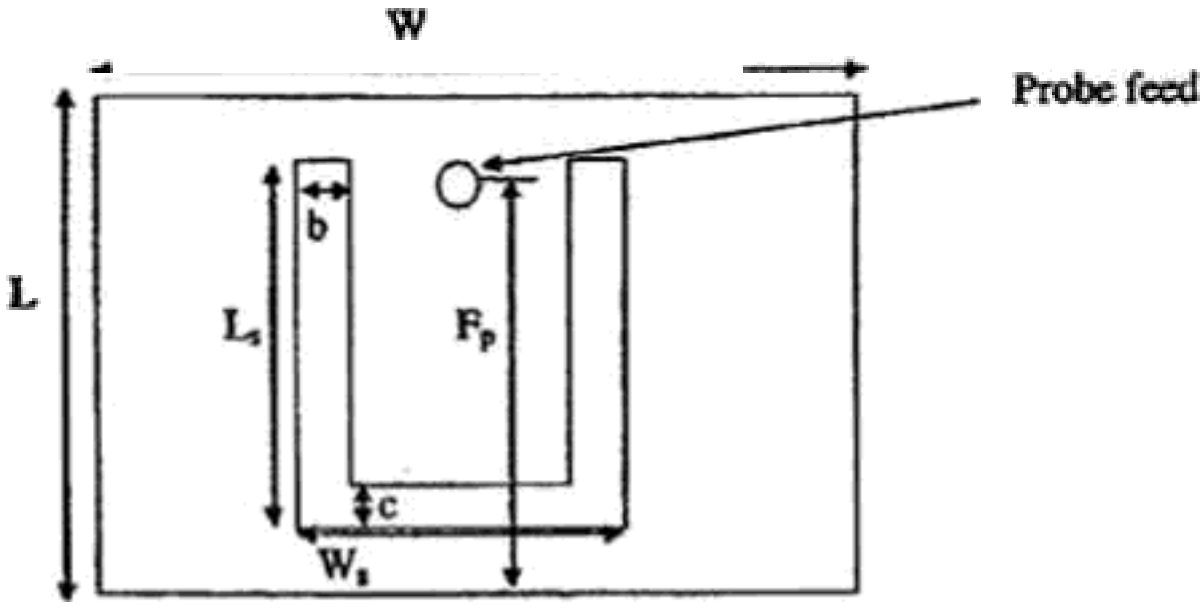

ig. 13.19 U-slot patch antenna.

'able 13.4(a). 900 MHz U-slot patches on microwave substrate (From [1

ε	Patch dimensions (cm)	Thickness (cm)	Normalized Area*	BW (%)
۱.0	21.97 × 12.45	2.69 ($0.081\lambda_o$)	.00	42
2.33	12.40 × 8.96	2.76 ($0.083\lambda_o$)	0.4!	26.5
۷	9.29 × 6.71	2.40 ($0.072\lambda_o$)	0.23	22.1
۳	5.74 × ۴..	2.01 ($0.060\lambda_o$)	0.087	14.4
۵				

Normalized with respect to the area of the U-slot patch in Huynh and Lee [1995]: 21.97 cm × 12.45 cm = 273.53 cm^2, $\varepsilon_r = 1.0$.

Table 13.4(b). Design parameters for 900 MHz U-slot patches on microwave substrate (all dimensions in cm). (From [11] © 2003 IEEE, Reprinted with permission.)

	$_r = 1.0$	$\varepsilon_r = 2.33$	ε_r 0	$\varepsilon_r = 9.8$
W	21.97 ($0.659\lambda_o$)	12.40 ($0.372\lambda_o$)	9.29 ($0.279\lambda_o$)	5.74 ($0.172\lambda_o$)
L	2.45 ($0.374\lambda_o$)	8.96 ($0.269\lambda_o$)	6.71 ($0.201\lambda_o$)	4.14 ($0.124\lambda_o$)
	6.86	4.82	3.6	2.^^
L_s	8.22	6.20	4.65	2.87
B	1.94	1.38	.03	0.64
C	0.89	0.69	0.52	0.32
F	6.22	4.48	3.36	3.04
T	2.69 ($0.081\lambda_o$)	2.76 ($0.083\lambda_o$)	2.40 ($0.072\lambda_o$)	2.01 ($0.060\lambda_o$)
D_{pro}	0.30	0.34	0.17	0.40

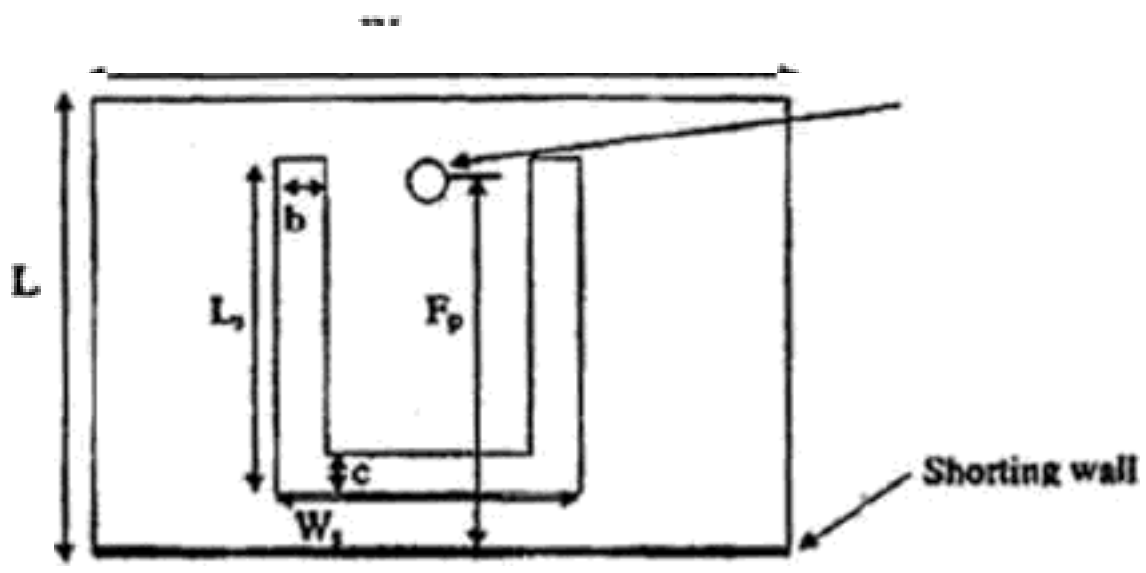

Fig. 13.20 U-slot patch antenna with a shorting wall

900 MHz. With the shorting wall, as ε_r increased from 1.0 to 4.0, the area of he patch was reduced by as much as 94%, while maintaining a bandwidth in excess of 20%. The design parameters for these antennas are presented in Table 13.5(b).

ble 13.5(a). 900 MHz U-slot patches on microwave substrate with shorting wall. (From [11] © 2003 IEEE, Reprinted with permission.)

ε_r	Patch dimensions (cm)	Thickness (cm)	Normalized Area*	BW (%)
1.0	8.14×8.14	2.71 ($0.081\lambda_o$)	0.2	22.7
2.33	5.71×5.7	3.02 ($0.091\lambda_o$)	0.12	22.6
4.0	3.97×3.97	3.62 ($0.109\lambda_o$)	0.05	27.9
9.8	2.66×2.66	2.68 ($0.080\lambda_o$)	0.025	14.7

*Normalized with respect to the area of the U-slot patch in Huynh and Lee [1995]: $21.97\,\text{cm} \times 12.45\,\text{cm} = 273.53\,\text{cm}^2$, $\varepsilon_r = 1.0$.

Table 13.5(b). Design parameters for 900 MHz U-slot patches on microwave substrate with shorting wall (all dimensions in cm). (From [11] © 2003 I Reprinted with permission.)

	$\varepsilon_r = 1.0$	$\varepsilon_r = 2.33$	$\varepsilon_r = 4.0$	$\varepsilon_r = 9.8$
W	8.14 ($0.244\lambda_o$)	5.71 ($0.171\lambda_o$)	3.97 ($0.119\lambda_o$)	2.66 ($0.0798\lambda_o$)
L	8.14 ($0.244\lambda_o$)	5.71 ($0.171\lambda_o$)	3.97 ($0.119\lambda_o$)	2.66 ($0.0798\lambda_o$)
W_o	4.88	3.43	2.38	1.6
	7.05	4.95	3.44	2.31
B	0.54	0.38	0.27	0.18
C	1.08	0.76	0.53	0.[illegible]
D	0.54	0.38	0.27	0.18
F	2.71	1.90	0.14	0.093
T	2.71 ($0.081\lambda_o$)	3.02 ($0.091\lambda_o$)	3.62 ($0.109\lambda_o$)	2.68 ($0.080\lambda_o$)
D_{probe}	0.27	0.25	0.28	0.19

3.3.1.3 *U-slot patch antenna with shorting pin*

he geometry of the U-slot patch antenna with a shorting pin is shown in igure 13.21.

he simulation results of such antennas designed for a center frequency of 900 MHz are shown in Table 13.6(a). The design parameters are given in Table 13.6(b). For the case of an air substrate, two sets of designs are given. In case 1, the patch area was 21% of the regular U-slot patch, and the impedance was 30%. In case 2, the patch area was only 5.6% of tne regular U-slot patch, and the impedance bandwidth was 15%. It should be noted that, in Figure 13, the shorting pin and the feed were placed at opposite sides of the patch. If the pin was placed close to the feed, which was the case for the rectangular patch (with no U-slot), the antenna did not function properly.

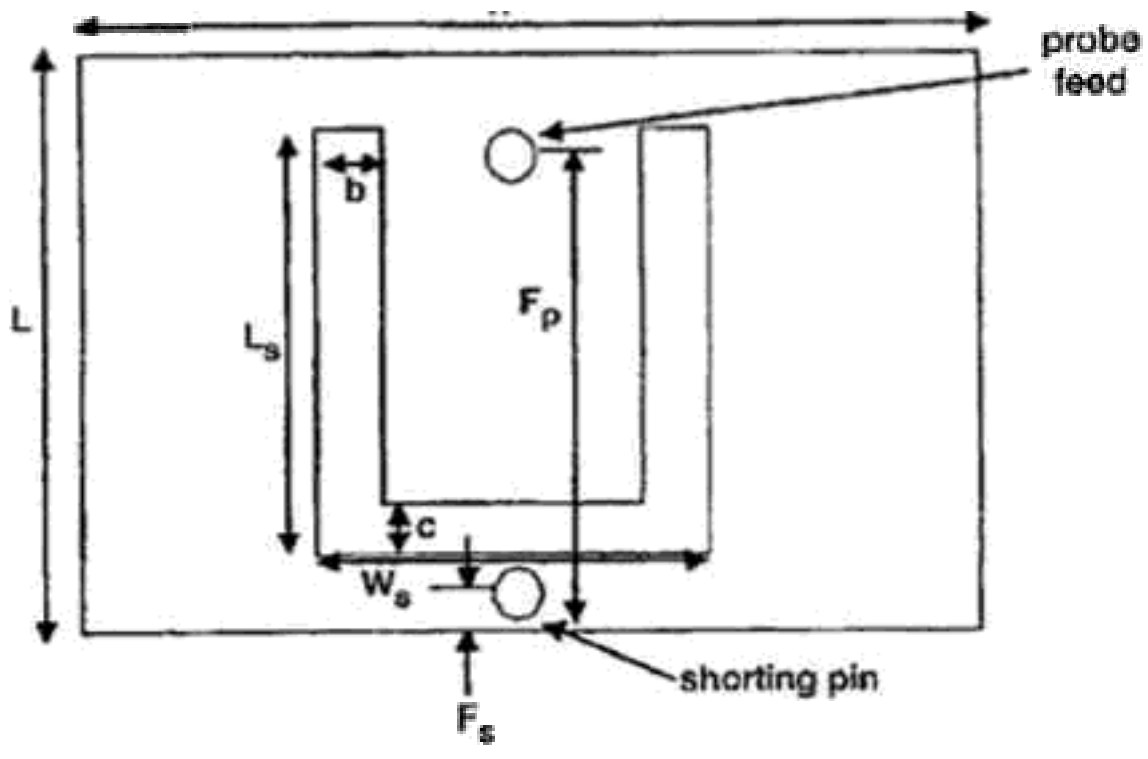

Fig. 13.21 U-slot patch antenna with shorting pin.

Table 13.6(a). 900 MHz U-slot patches with shorting pins. (From [11] © 200 EEE. Reprinted with permission.)

ε_r	Patch dimensions (cm)	Thickness cm)	ormalized Area	BW (%)
.0	(1) 8.4 × 7.0	2.8 (0.084λ_o)	0.21	30
.0	(2) 5.33 × 3.9	3.3 (0.099λ_o)	0.056	5
3.27	2.84 × 2.08	3.6 (0.108λ_o)	0.022	10
4.0	2.84 × 2.	3.3 (0.099λ_o)	0.022	1

Normalized with respect to the area of the U-slot patch in Huynh and Lee [1995]: 21.97 cm × 12.45 cm = 273.53 cm^2, $\varepsilon_r = 1.0$.

able 13.6(b). Design parameters for 900 MHz U-slot patches with shorting pin (all dimensions in cm). (From [11] © 2003 IEEE, Reprinted with permission.)

	$\varepsilon_r = 1.0$ (1)	$_r = 1.0$ (2)	$\varepsilon_r = 3.27$	$\varepsilon_r = 4.5$
W	8.4 (0.252λ_o)	5.33 (0.016λ_o)	2.84 (0.00852λ_o)	2.84 (0.00852λ_o)
L	7.0 (0.210λ_o)	3.9 (0.012λ_o)	2.08 (0.00624λ_o)	2.08 (0.00624λ_o)
$W_$	7.47	1.8	0.96	0.96
L_s	4.67	2.93	1.22	22
B	2.1	0.65	0.68	0.98
C	0.47	0.32	0.17	0.17
$_P$	6.8	3.6	1.98	1.88
F_s	0.47	0.075	0.3	0.98
d_p	0.47	0.3	0.2	0.4
d_s	0.93	0.15	0.68	0.49
T	2.8 (0.084λ_o)	3.3 (0.099λ_o)	3.6 (0.108λ_o)	3.3 (0.099λ_o)

The typical simulated radiation patters of a U-slot patch antenna with shorting pin are shown in Figure 13.22.

13.3.1.4 *Half-structures*

A. Half U-Slot Patch Antenn

It was suggested by Deshmukh and Kumar [14] that removing half of the U-slot patch along the line of symmetry still resulted in a broadband antenna. Figure 13.23 shows the simulated current distribution of the full and half structures. It is seen that the current paths in the two patches, and hence their resonant behaviors, are similar.

s an example, consider the U-slot patch antenna of Huynh and Lee [15]. The simulated return loss curves for the full structure and the half structure

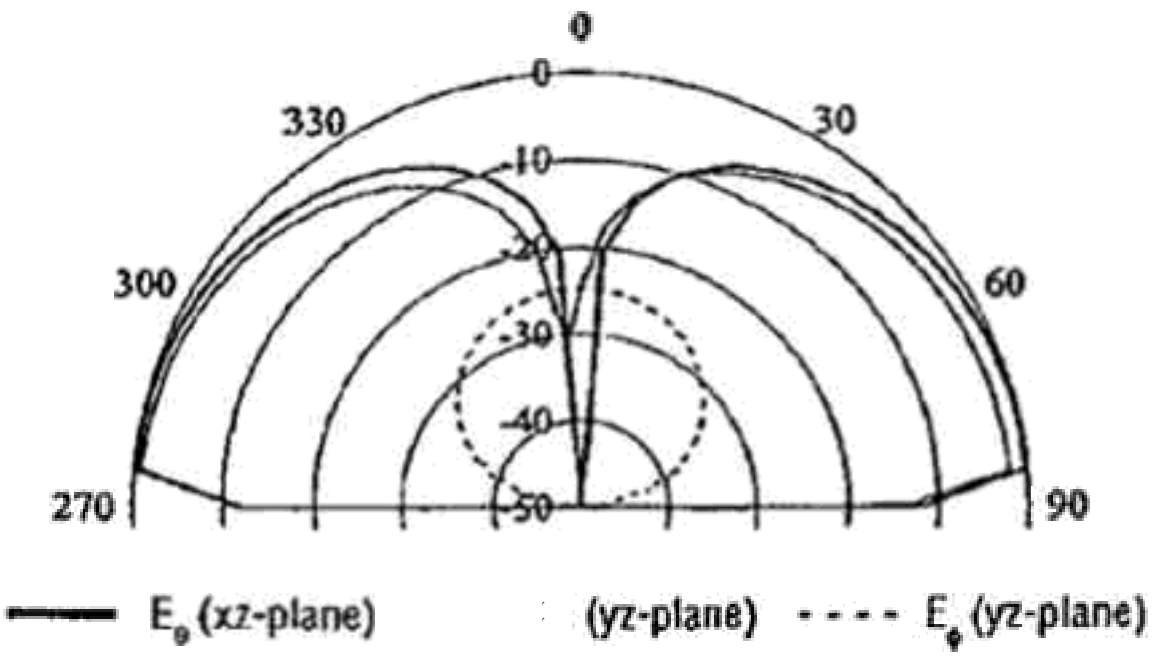

Fig. 13.22 Simulated radiation patterns of the U-slot patch antenna with shorting pin at 0.85 GHz (10 dB/div).

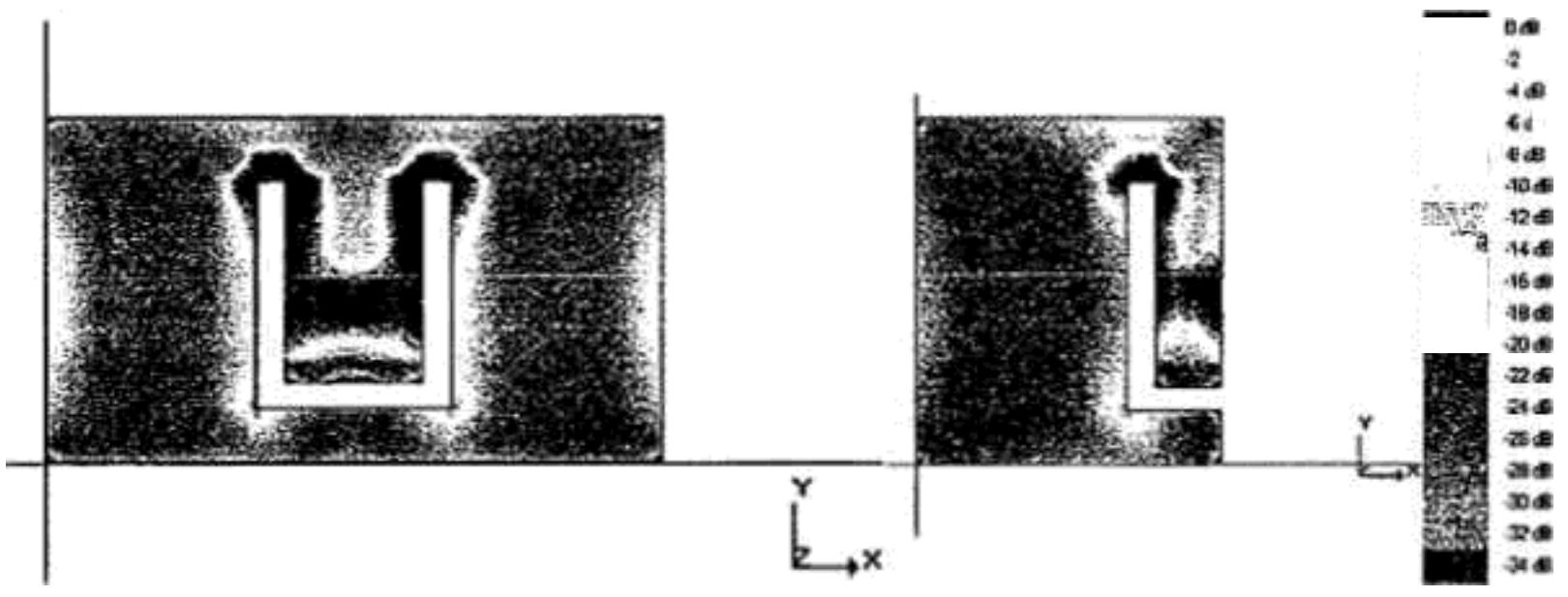

Fig. 13.23 Simulated current distributions in (a) Full U-slot patch; (b) Half U-slot patch (From [17] © 2005 IEEE, Reprinted with permission.)

are shown in Figure 13.24. The bandwidth of the former is 35% and that of the latter is 28.6%. The radiation patterns are shown in Figure 13.25 is seen that, due to its asymmetry, the cross polarization level of t half-structure is very high.

ıe half-structure idea was applied to the U-slot patch with shorting wall [16] and the U-slot patch with shorting pin [17]. These designs ar described below.

B. Half U-Slot Patch with Shorting Wall

Figure 13.26(a) shows the geometry of the half U-slot patch antenna with shorting wall, obtained from cutting away half of the full U-slot patch ant a (Figure 13.26(b)) along the line of symmetry. The feed wire was 1 mm in diameter. Measured and simulation results of SWR are shown in

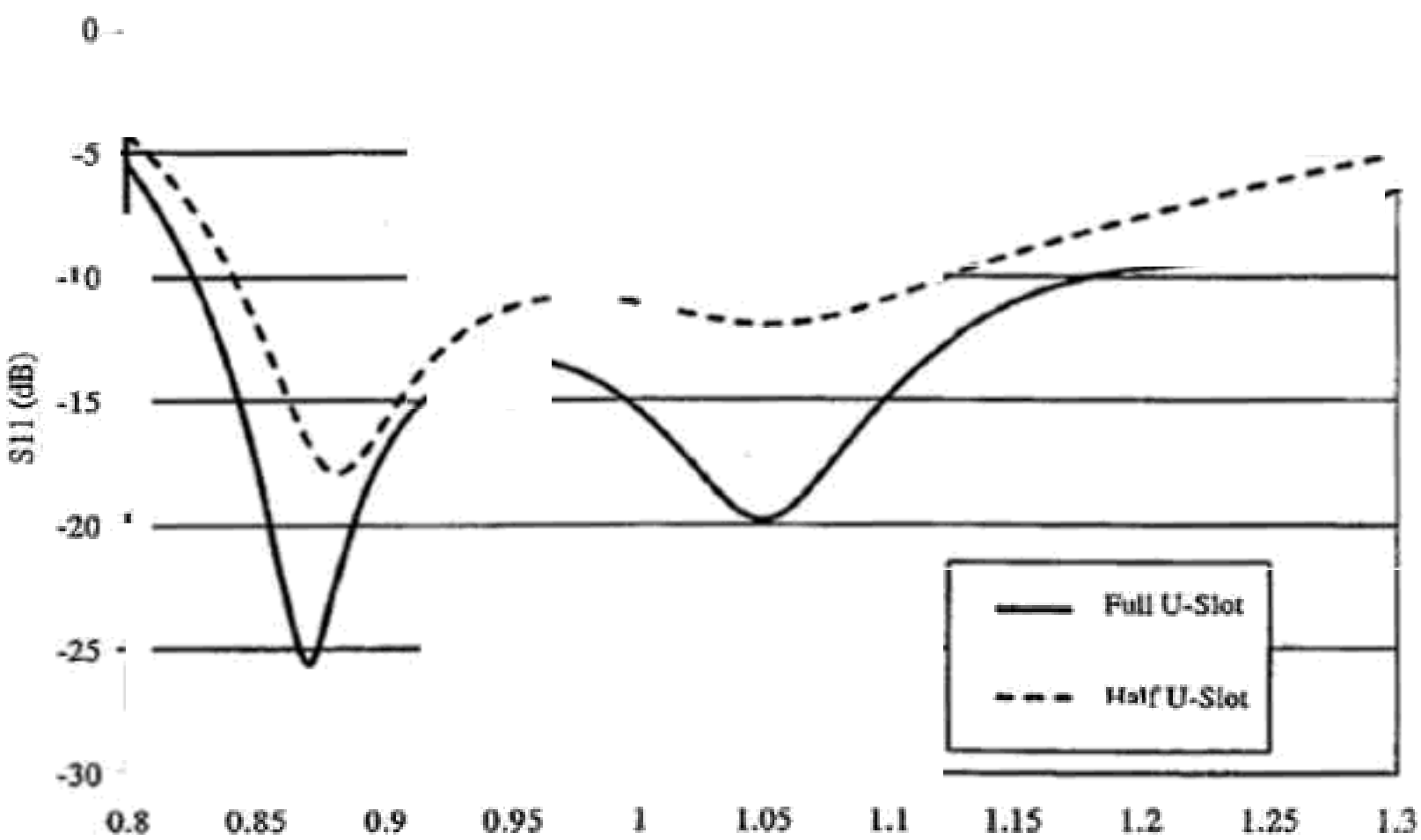

uency (GHz)

	Half U-slot	Full U-slot
Freq. range	0.84GHz–1.12GHz	0.83GHz–1.18GHz
BW	28.6%	35%

Fig. 13.24 Simulated return loss of the full U-slot patch of Huynh and Lee [15] and the half structure obtained by removing half of the U-slot patch along the line of symmetry.

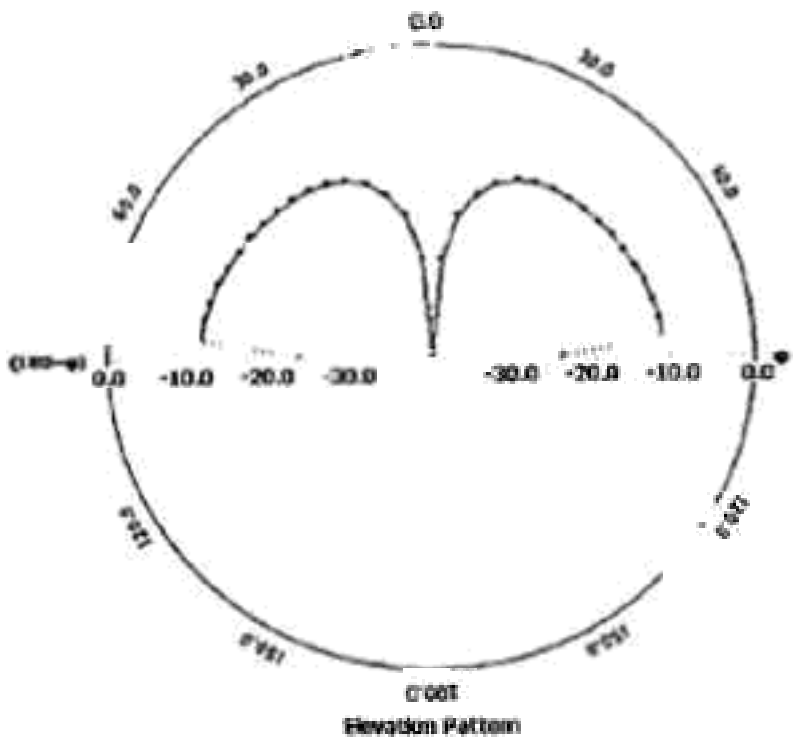

(a)

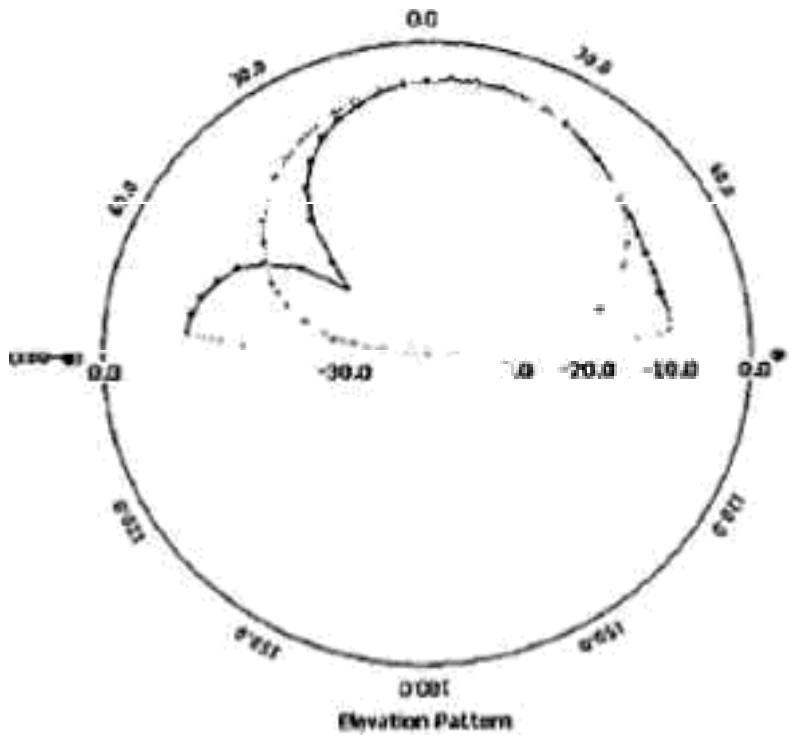

(b)

ig. 13.25 Simulated radiation patterns of the antennas of Figure 13.24 at 1 GHz.(a) Full U-slot, and (b) half U-slot.

Figure 13.27. The measured and simulated bandwidths were 28.5% and 23% respectively, both centered at 2.6 GHz. The measured gain was around 2 dBi across the operating band. Measured patterns at 2.6 GHz are shown in Figure 13.28.

'ith the radiation introduced from the feeding wire and the shorting wall, both E_θ in the x-z plane and $E\phi$ in the y-z plane had similar radiation level. In addition, the radiation from the shorting wall leds to a dip in the pattern of E_θ in the y-z plane. The radiation patterns were stable. These results showed that the half-U-quarter-wave patch had similar performance characteristics as the full-U-quarter-wave patch [12].

C. Half U-Slot Patch with Shorting Pin

'igure 13.29 shows the geometries of the half and full U-slot patch antennas with shorting pins. The former is formed by cutting away half of the f U-slot patch along the line of symmetry. The radii of the shorting pin and 'ne probe feed were 4.65 and 2 mm respectively.

Figure 13.30 shows the measured and simulated SWRs of the half and full U-slot patch antennas with shorting pin. The center frequency of the half structure was 40 MHz (4.7%) higher than the full structure. The match-'ng frequency range of the half U-slot patch antenna was from 0.81 to 0.99 GHz with an impedance bandwidth of 20%, where the area of the half U-slot patch was only $0.0273\lambda^2$. The full U-slot patch was matched from 0.75 to 0.97 GHz with an impedance bandwidth of 25.6%.

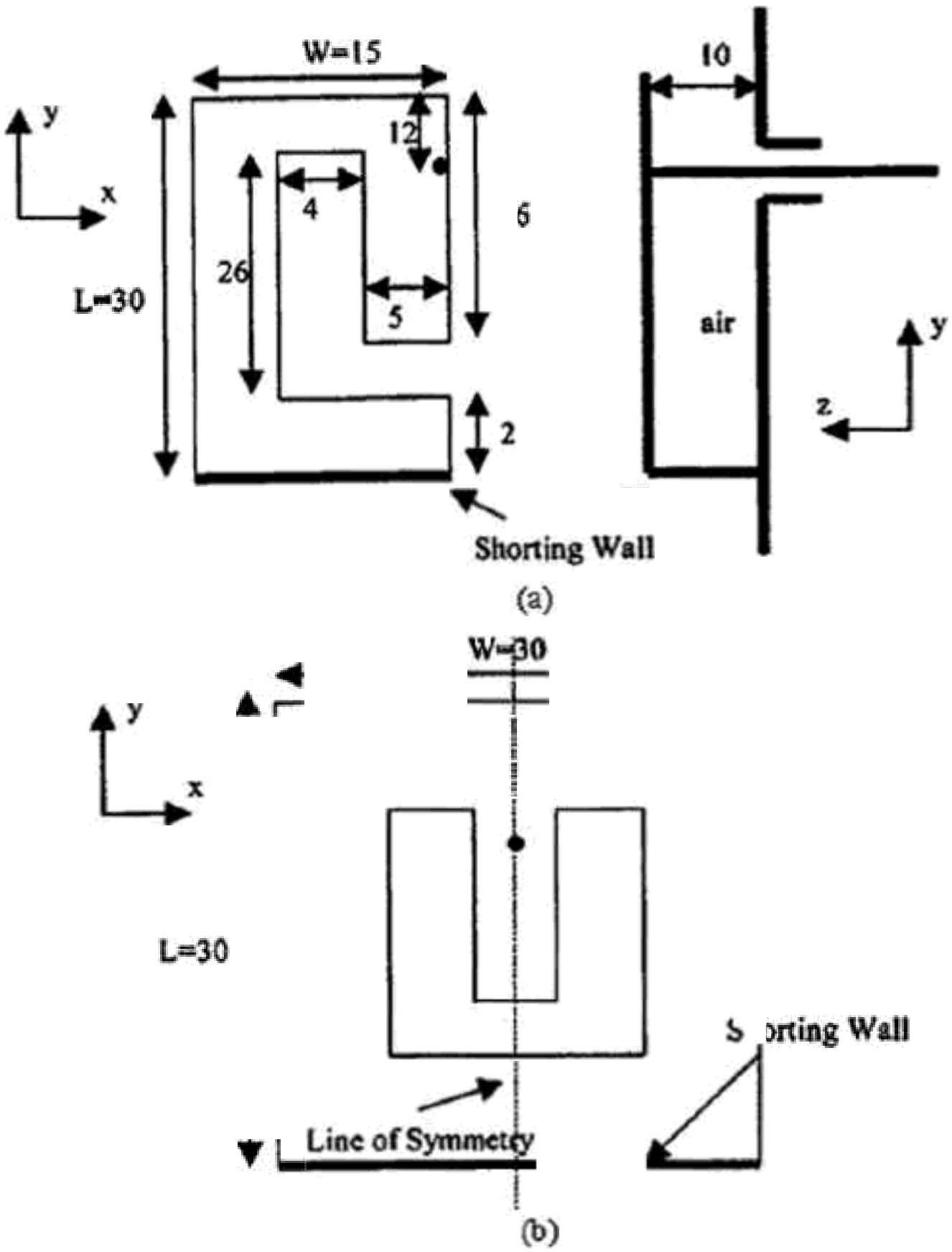

Fig. 13.26 Geometries of the U-slot patch antennas with shorting wall (units in mm and not to scale). (a) Half U-slot. (b) Full U-slot. (From [16] © 2003 IEEE, Reprinted with permission.)

Figure 13.31(a) and (b) shows the simulated radiation patterns of the half and full U-slot patch antenna with shorting pin at 0.9 GHz, respectively. Simulation results were modeled in an infinite ground environment. The radiation due to the vertical components (shorting pin and feeding probe) increased the radiation level of E_θ in the y-z plane. However, two radiating edges of the half U-slot patch radiated, which gave more symmetric

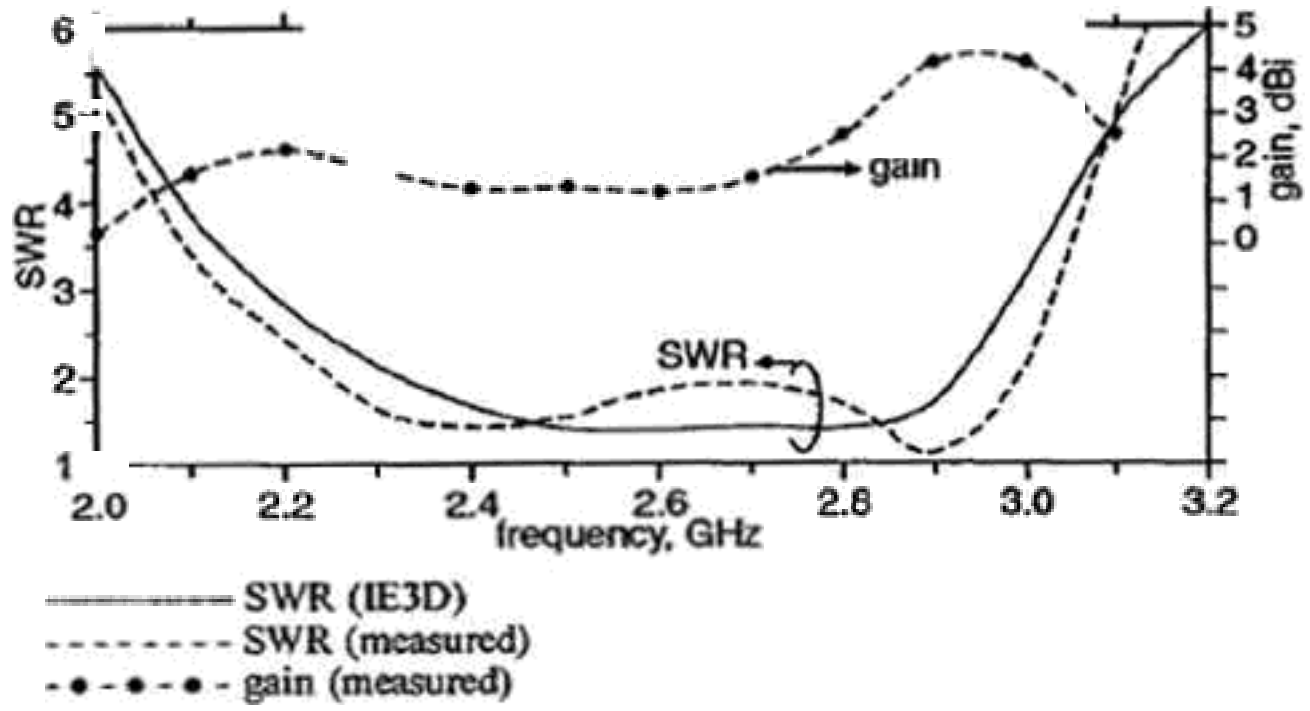

Fig. 13.27 SWR and gain of the half U-slot patch antenna of Figure 13.23(a). (From [16] © 2003 IEEE, Reprinted with permission.)

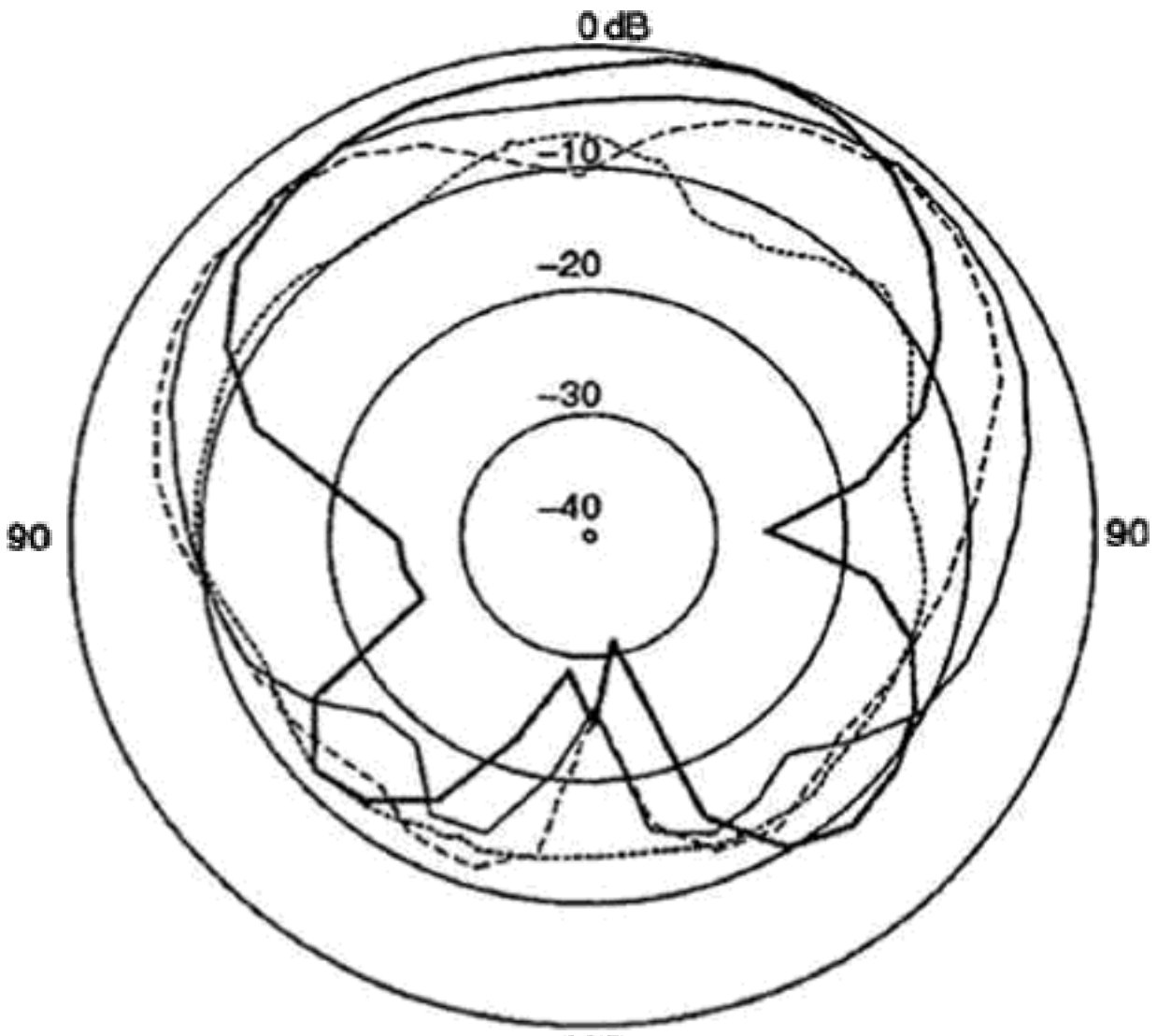

Fig. 13.28 Measured radiation patterns at 2.6 GHz (10 dB/div). (From [13] © 2006 IEEE, Reprinted with permission.)

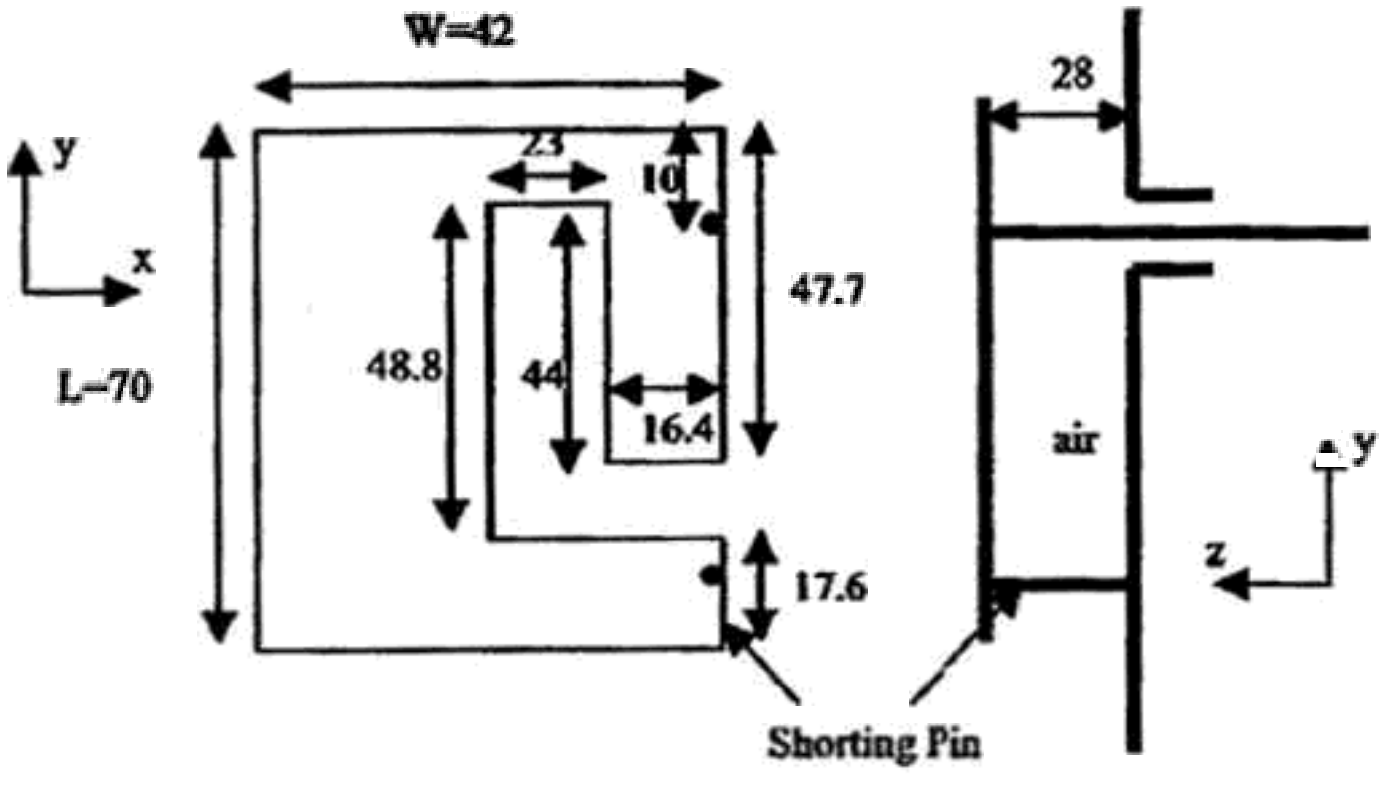

Fig. 13.29 Geometries of the U-slot patch antennas with shorting pin (units in mm and not to scale). (a) Half U-slot. (b) Full U-slot. (From [17] © 2005 IEEL, Reprinted with permission.)

radiation patterns along the y-z plane than the half U-slot patch with shorting wall [15]. In addition, slightly asymmetrical pattern was obtained in the x-z plane and the higher level of the E_ϕ field in the y-z plane is due to the asymmetrical structure of the half U-slot antenna. The E_ϕ field is cancelled out in the y-z plane of the full U-slot antenna with its symmetrical geometry.

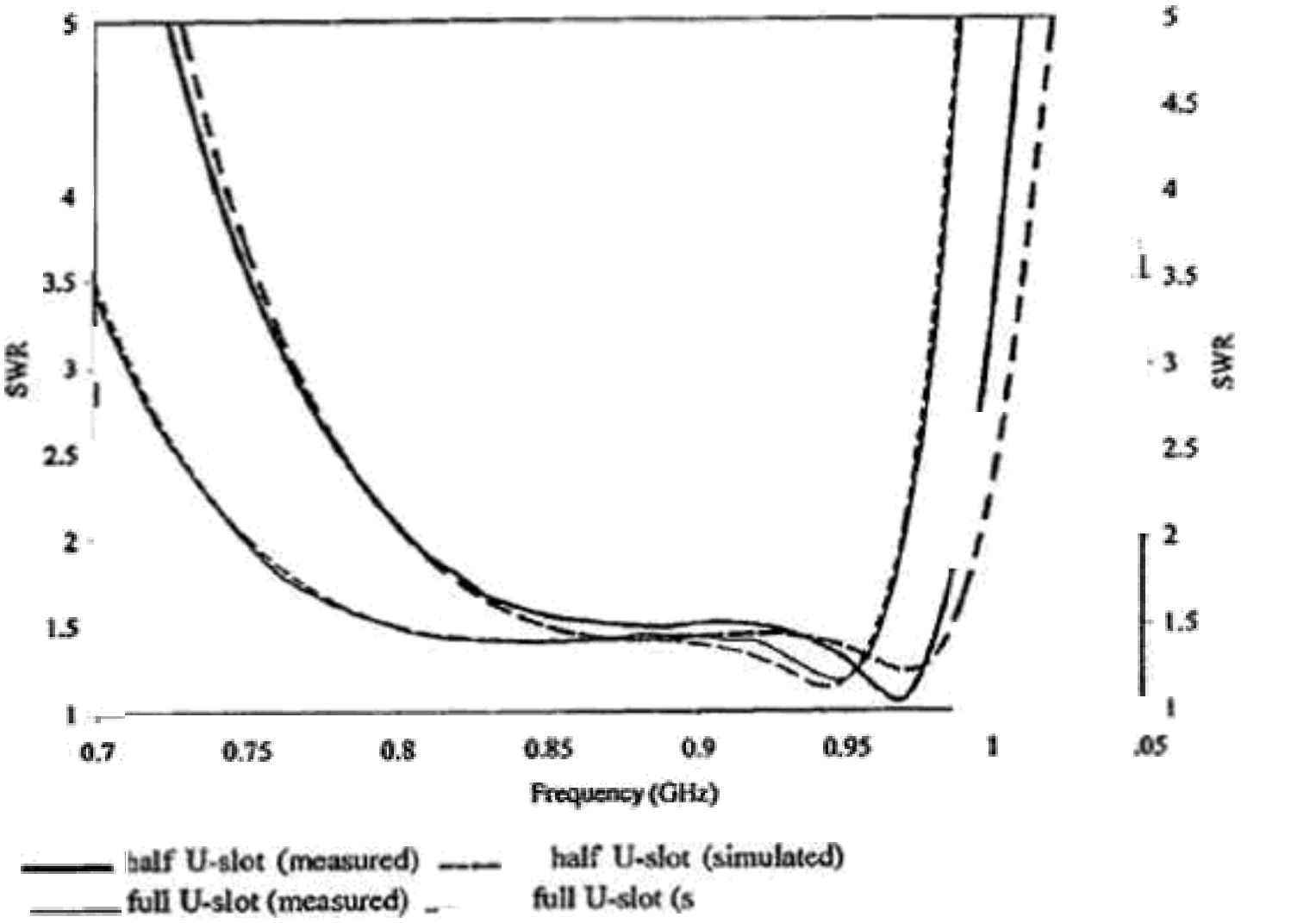

13.30 Measured and simulated SWR of the U-slot patch antennas with shorting pin. (From [17] © 2005 IEEE, R printed with permission.)

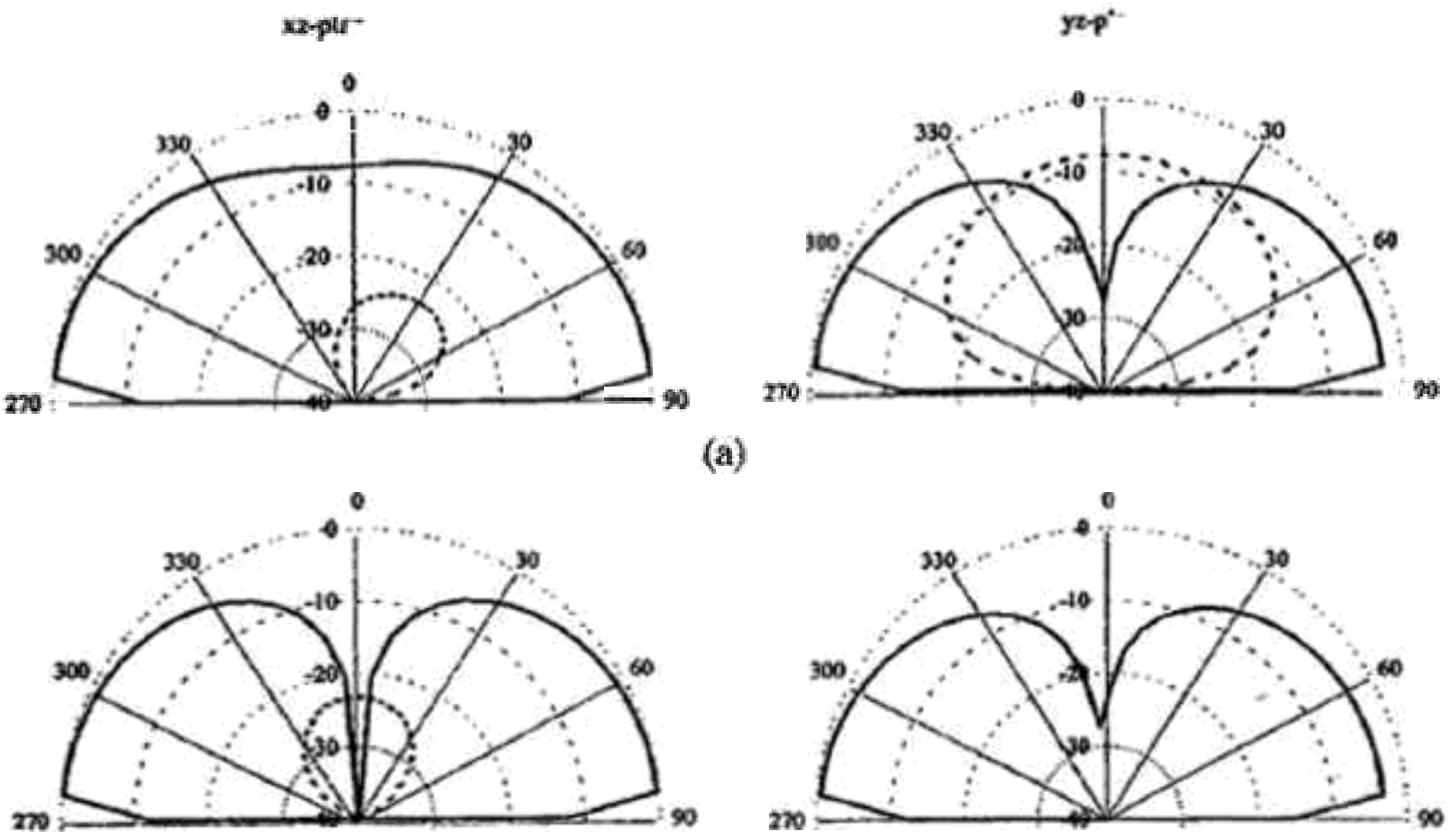

Fig. 13.31 Simulated radiation patterns of the U-slot patch antenna with shor ing pin at 0.9 GHz (10 dB/div). (a) Half U-slot. (b) Full U-slot. E_θ, E_ϕ. (From [17] © 2005 IEEE, Reprinted with permission.)

'able 13.7. Comparison between the full _ half U-slot pat :h antennas (all mensions in mm). (From [17] © 2005 IEEE, R_ _ permission.)

		U-slot patch with shorting wall [15]		_ slot patch with shorting pin	
		Full	Half	Full	Half
Dimensions	L	30 ($0.24\lambda_o$)	20 ($0.26\lambda_o$)	($0.2\lambda_o$)	70 ($0.21\lambda_o$)
	W	30 ($0.24\lambda_o$)	15 ($0.13\lambda_o$)	84 ($0.24\lambda_o$)	42 ($0.13\lambda_o$)
	H	20 ($0.08\lambda_o$)	10 ($0.09\lambda_o$)	28 ($0.08\lambda_o$)	28 ($0.08\lambda_o$)
Size		$0.0576\lambda_o^2$	$0.0338\lambda_o^2$	$0.048\lambda_o^2$	$0.0273\lambda_o^2$
Bandwidth (SWR < 2		28.1%	28.6%	25.6%	20%
Size reductio_			%	43%	

'able 13.7 summarizes the com_ _ison between the full and half U-slot patch antennas.

13.3.2 *The L-probe Technique*

3.3.2.1 *The two-layer L-probe-fed patch antenna*

The use of the L-probe feed to broaden the bandwidth of patch antennas was discussed in Chapter 11. The design requires the horizontal arm of the feed probe be embedded within the substrate material, making it difficul_ to use any material other than foam or air for the substrate. To realize the goal of reducing the resonant length of the L-probe patch by increasing the substrate dielectric constant, a two-layer configuration was conceived, as shown in Figure 13.32.

By placing a microwave substrate in the region between the conducting patch and the L-probe, and foam or air between the ground plane and the

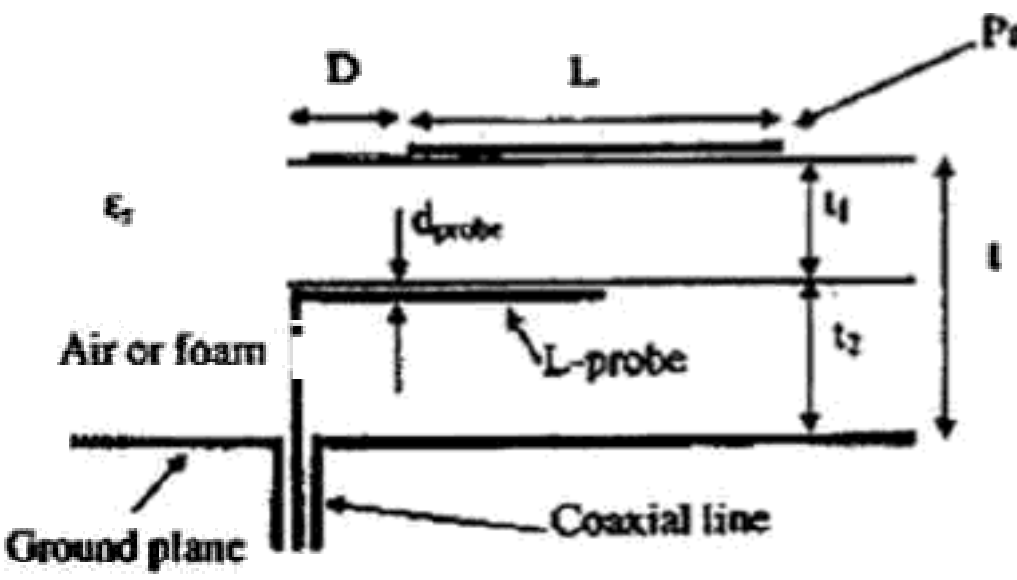

'ig. 13.32 Two-layer L-probe patch antenna.

Table 13.8(a). 900 MHz L-probe patch. (From [11] © 2005 IEEE, Reprinted with permission.)

ε_r	Patch dimensions (cm)	Thickness (cm)	Normalized Area*	BW (%)
1.0	15.83 × 13.19	3.48 ($0.104\lambda_o$)	1.0	40
2.32	12.43 × 10.36	4.06 ($0.122\lambda_o$)	0.62	40.6
4.2	9.75 × 8.12	3.90 ($0.117\lambda_o$)	0.38	38.3
9.8	7.52 × 6.26	3.78 ($0.143\lambda_o$)	0.23	38.1

*Normalized with respect to the L-probe patch: 15.83 cm × 13.19 cm = 208.8 cm^2, $\varepsilon_r = 1.0$.

Table 13.8(b). Design parameters for 900 MHz L-probe patches (all dimensions in cm). (From [11] © 2005 IEEE, Reprinted with permission.)

	$\varepsilon_r = 1.0$	$\varepsilon_r = 2.32$	$\varepsilon_r = 4.2$	$\varepsilon_r = 9.8$
W	15.83 ($0.475\lambda_o$)	12.43 ($0.373\lambda_o$)	9.75 ($0.293\lambda_o$)	7.52 ($0.226\lambda_o$)
L	13.19 ($0.396\lambda_o$)	10.36 ($0.311\lambda_o$)	8.12 ($0.244\lambda_o$)	6.26 ($0.188\lambda_o$)
L_h	5.54	4.35	3.41	2.63
D	1.06	8.28	6.50	5.0
t_1		1.28	1.72	3.10
t_2		2.78	2.18	0.68
$t = t_1 + t_2$	3.48 ($0.104\lambda_o$)	4.06 ($0.122\lambda_o$)	3.90 ($0.117\lambda_o$)	3.78 ($0.143\lambda_o$)
d_{prob}	0.53	0.4	0.33	0.25

L-probe, the effective permittivity of the region is increased compared to that of foam or air. This reduces the resonant length of the patch, without increasing the difficulty of fabrication, since the horizontal arm of the L-probe lies in the air or foam layer.

Table 13.8(a) shows the simulation results obtained using Ansoft Ensemble software for several values of ε_r, designed at a center frequency of 900 MHz. The normalized area column of the Table uses the area of the $\varepsilon_r = 1.0$ case as a reference. It is seen that, as ε_r increase, the size reduction is similar to the U-slot patches, but the bandwidth is significantly larger, as is the substrate thickness. Table 13.8(b) shows the design parameters for these antennas.

13.3.2.2 *The two-layer L-probe-fed patch antenna with a shorting wall*

To further reduce the area of the patch, a shorting wall is added. As shown in Figure 13.33.

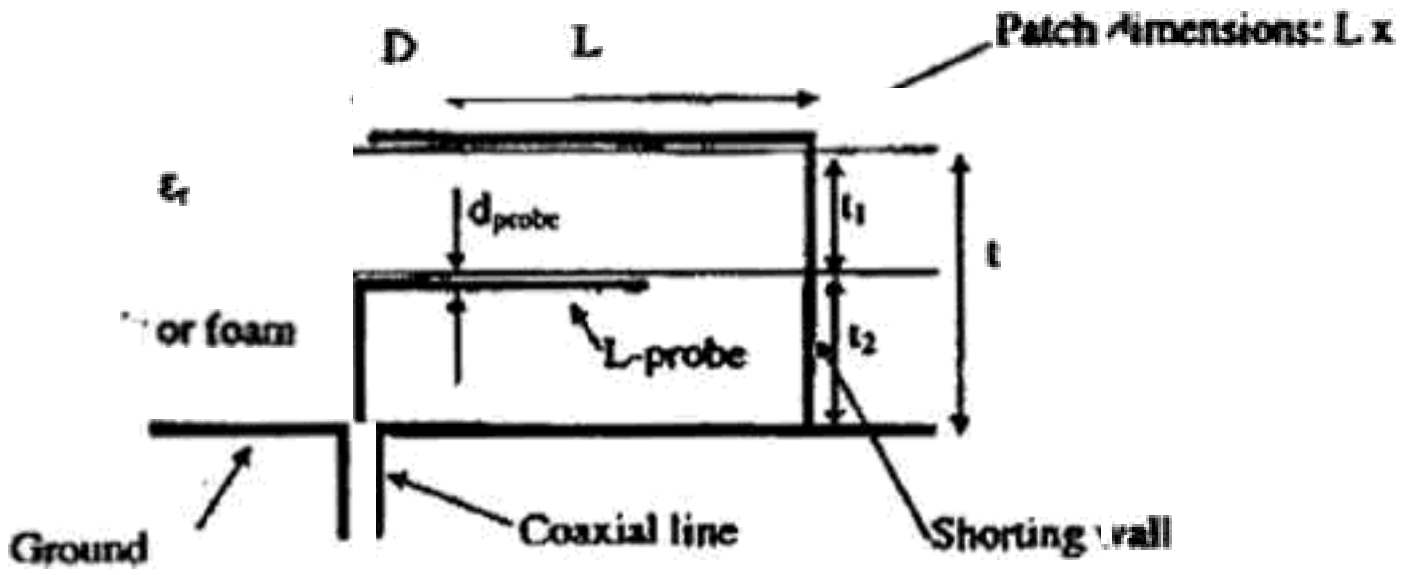

Fig. 13.33 Two-layer L-probe patch antenna with shorting wa.

Table 13.9(a) shows the simulation results for four cases, all designed for a center frequency of 900 MHz. By adding the shorting wall to the $\varepsilon_r = 1.0$ case, tne area is reduced by almost half. As the dielectric constant of the upper [illegible] creased, the size of the patch decreases. For the $\varepsilon_r = 2.33$ case, the area is reduced by 76%. For the $\varepsilon_r = 4.0$ and 9.8 cases, the area is reduced by 88% and 93% respectively, when compared to the L-probe antenna with $\varepsilon_r = 1.0$ and no shorting wall. The impedance bandwidths of the antenna remain above 20% for all four cases by using thick substrate ($0.07\lambda_o - 0.13\lambda_o$). Detail design parameters are given in Table 13.9(b).

13.3.3 *Shorted Stacked Patches*

13.3.3.1 *Stacked patches with shorting walls*

As discussed in Chapter 9, the use of stacked patches is an effective metho of obtaining wide impedance bandwidth. Both the shorting wall and tne shorting pin size reduction techniques can be applied to reduce the size of acked patches.

Table 13.9(a). 900 MHz L-probe patches with shorting walls.

ε_r	Patch dimensions (cm)	Thickness (cm)	Normalized Area*	BW (%)
1.0	17.0×6.82	4.26 ($0.128\lambda_o$)	0.56	29.6
2.33	11.3×4.52	3.61 ($0.108\lambda_o$)	0.24	45.1
4.0	7.92×3.1	3.65 ($0.110\lambda_o$)	0.12	36.2
9.8	5.97×2.39	2.34 ($0.070\lambda_o$)	0.068	22.

*Normalized with respect to the L-probe patch: $15.83\,\text{cm} \times 13.19\,\text{cm} = 208.8\,\text{cm}^2$, $\varepsilon_r = 1.0$.

Table 13.9(b). Design parameters for 900 MHz L-probe patches with shorting walls(all dimensions in cm).

	$\varepsilon_r = 1.0$	$\varepsilon_r = 2.33$	$\varepsilon_r = 4.0$	$\varepsilon_r = 9.8$
W	17.0 ($0.510\lambda_o$)	10.3 ($0.339\lambda_o$)	7.92 ($0.238\lambda_o$)	5.97 ($0.179\lambda_o$)
L	6.82 ($0.205\lambda_o$)	5.52 ($0.136\lambda_o$)	3.17 ($0.095\lambda_o$)	2.39 ($0.072\lambda_o$)
L_p	6.53	4.33	3.04	2.29
D	1.14	0.75	0.53	0.40
t_1		1.17	1.10	1.06
t_2		2.45	2.24	1.28
$t = t_1 + t_2$	4.29 ($0.128\lambda_o$)	3.61 ($0.108\lambda_o$)	3.65 ($0.110\lambda_o$)	2.34 ($0.070\lambda_o$)
d_{probe}	0.38	0.38	0.26	0.20

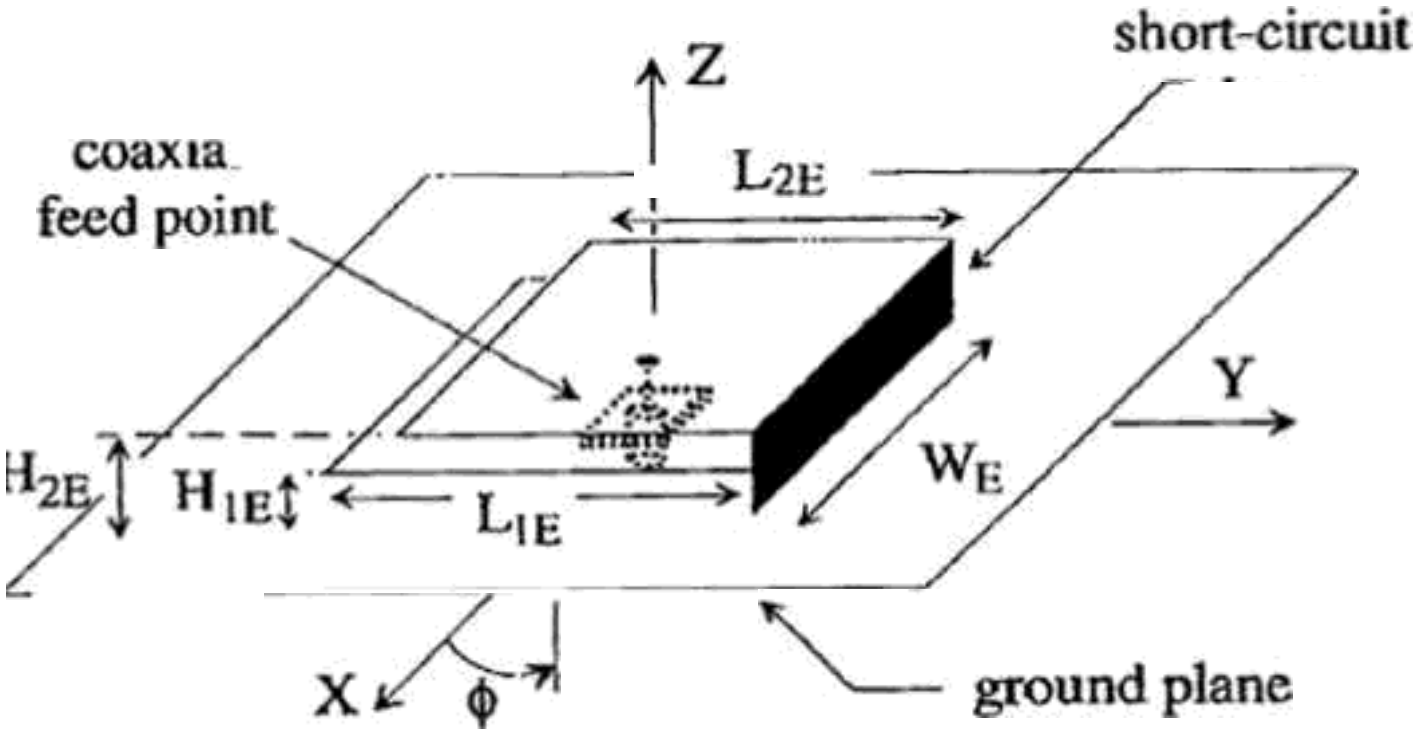

Fig. 13.34 Geometry of the shorted stacked patch antenna on air substrate. $W_E = 35$ mm, $L_{1E} = 35$ mm, $L_{2E} = 25$ mm (From [18] © 1999 IEEE, Reprinted with permission.)

Said *et al.* [18] studied the stacked patch on air substrate, with a shorting wall shown in Figure 13.34.

The measured impedance bandwidth as a function of the thickness of the two layers are given in Table 13.10. For case (4) measured and simulated VSWR versus frequency are shown in Figure 13.35 and the bandwidth was almost 30%.

13.3.3.2 *Stacked patches with shorting pins*

In using shorting pins to reduce the sizes of stacked patches, it was found that, if one pin was used, only 10% bandwidth was achieved [19].

Table 13.10. Impedance bandwidth versus height of the shorted stacked patch antenna. (From [18] © 1999 IEEE, Reprinted with permission.)

H_{1E}	H_{2E}	Bandwidth (VSWR < 2)
3 mm	5 mm	15.4%
3 mm	5.5 mm	18.6%
4 mm	7 mm	23%
5.5 mm	10.5 mm	29.5%

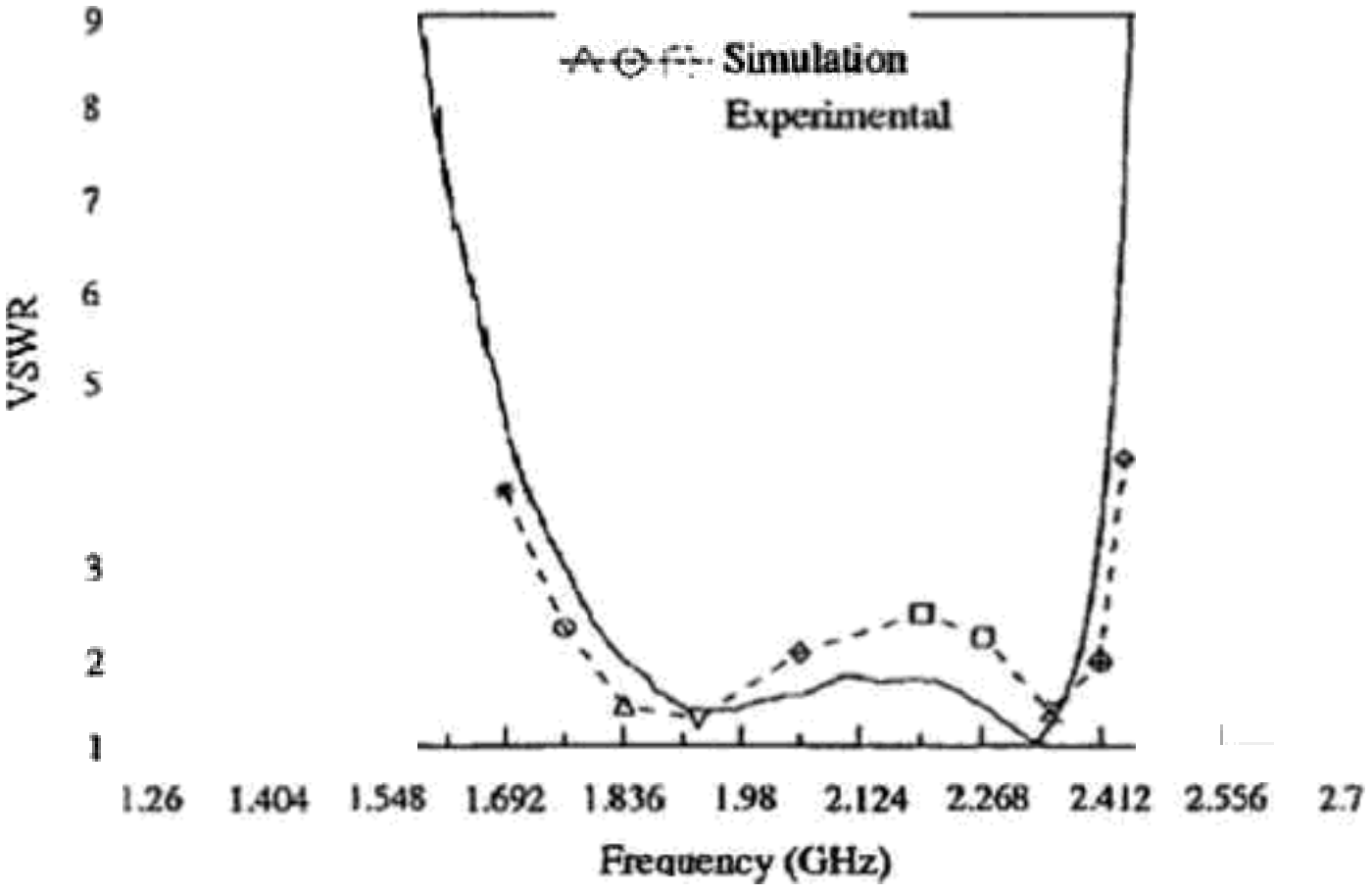

Fig. 13.35 Measured and simulated VSWR versus frequency of the antenna of Figure 13.34. (From [18] © 1999 IEEE, Reprinted with permission.)

In order to achieve wider bandwidth, it was necessary to use two shorting pins, one connecting the upper and lower patches and another connecting the top patch to the ground plane through the lower patch, as shown in Figure 13.36 [20]. This design was tested experimentally for the case of foam substrates in both the upper and lower layers. An impedance bandwidth of 34% was reported, with the longest dimension of the patches about $0.19\lambda_o$, where λ_o is the wavelength at the center frequency of about 1.7 GHz. The total antenna thickness was $0.1\lambda_o$. The detailed parameters and the measured and predicted input impedance response were shown in Figure 13.37. The measured radiation patterns are show

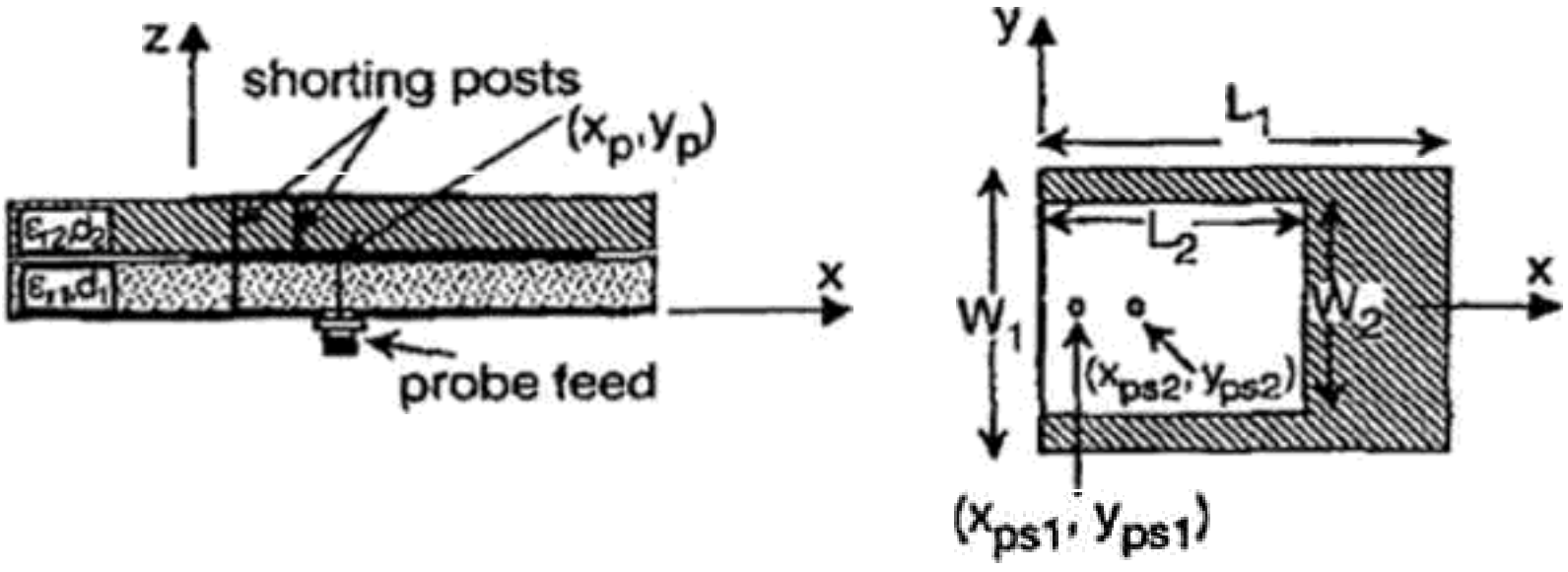

ig. 13.36 Schematic of the stacked patch with two shorting pins. Radius of coaxial probe = r_o, Radius of shorting pin 1 = r_{os1}, Radius of shorting pin 2 = r_{os2}. (From [20] © 1998 IET, Reprinted with permission.)

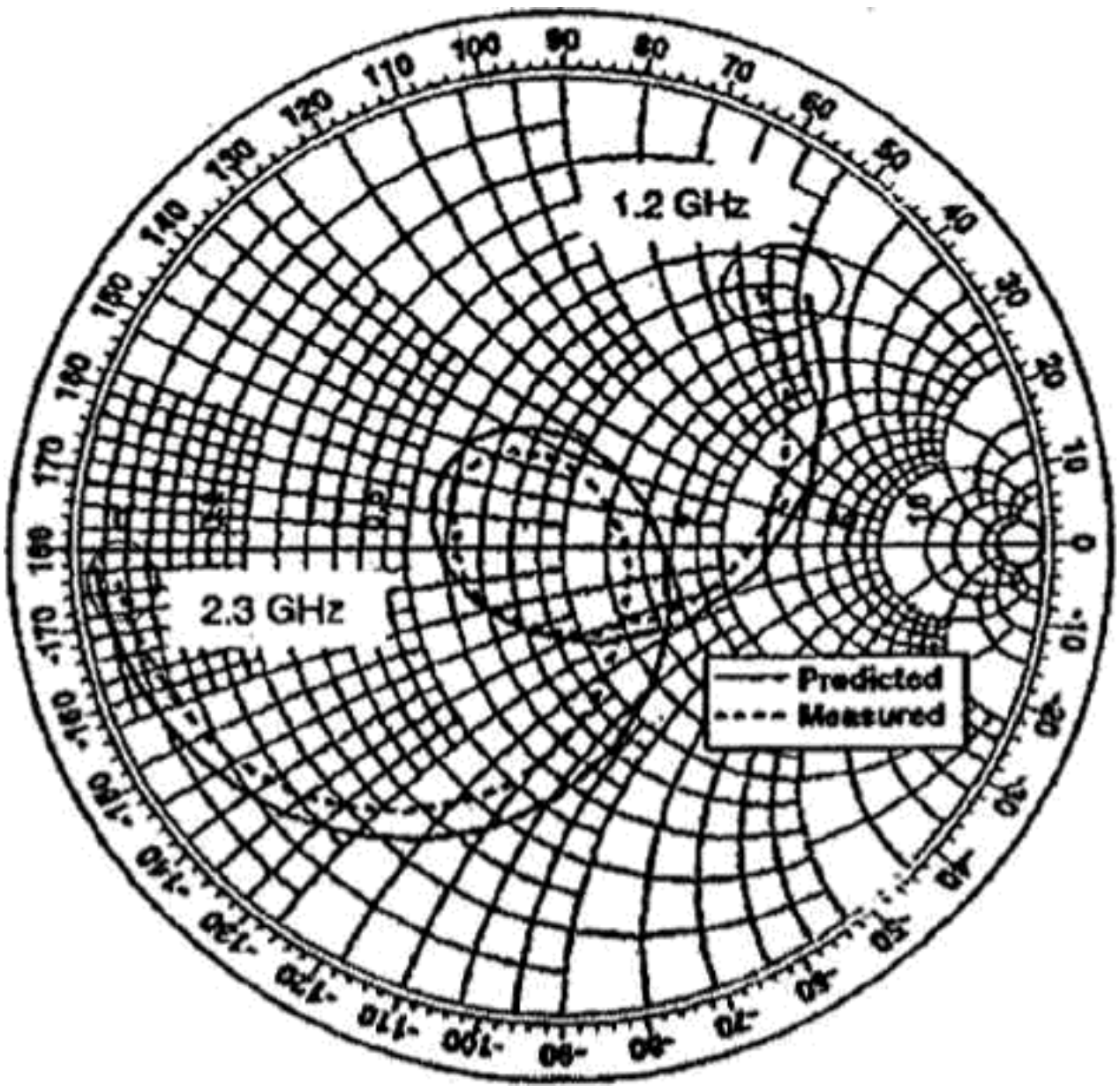

ig. 13.37 Predicted and measured input impedance response of the stacked patch with two shorting pins with parameters: $e_{r1} = e_{r2} = 1.07$, $d_1 = 2.0\,\text{mm}$, $d_2 = 18.0\,\text{mm}$, $L_1 = 36.0\,\text{mm}$, $W_1 = 23.0\,\text{mm}$, $L_2 = W_2 = 23.0\,\text{mm}$, $x_p = x_{ps2} = 15.0\,\text{mm}$, $r_0 = r_{0s2} = 0.325\,\text{mm}$, $x_{ps1} = 1.0\,\text{mm}$, $r_{0s2} = 0.6\,\text{mm}$, ____ predicted, neasured. (From [20] © 1998 IET, Reprinted with permission.)

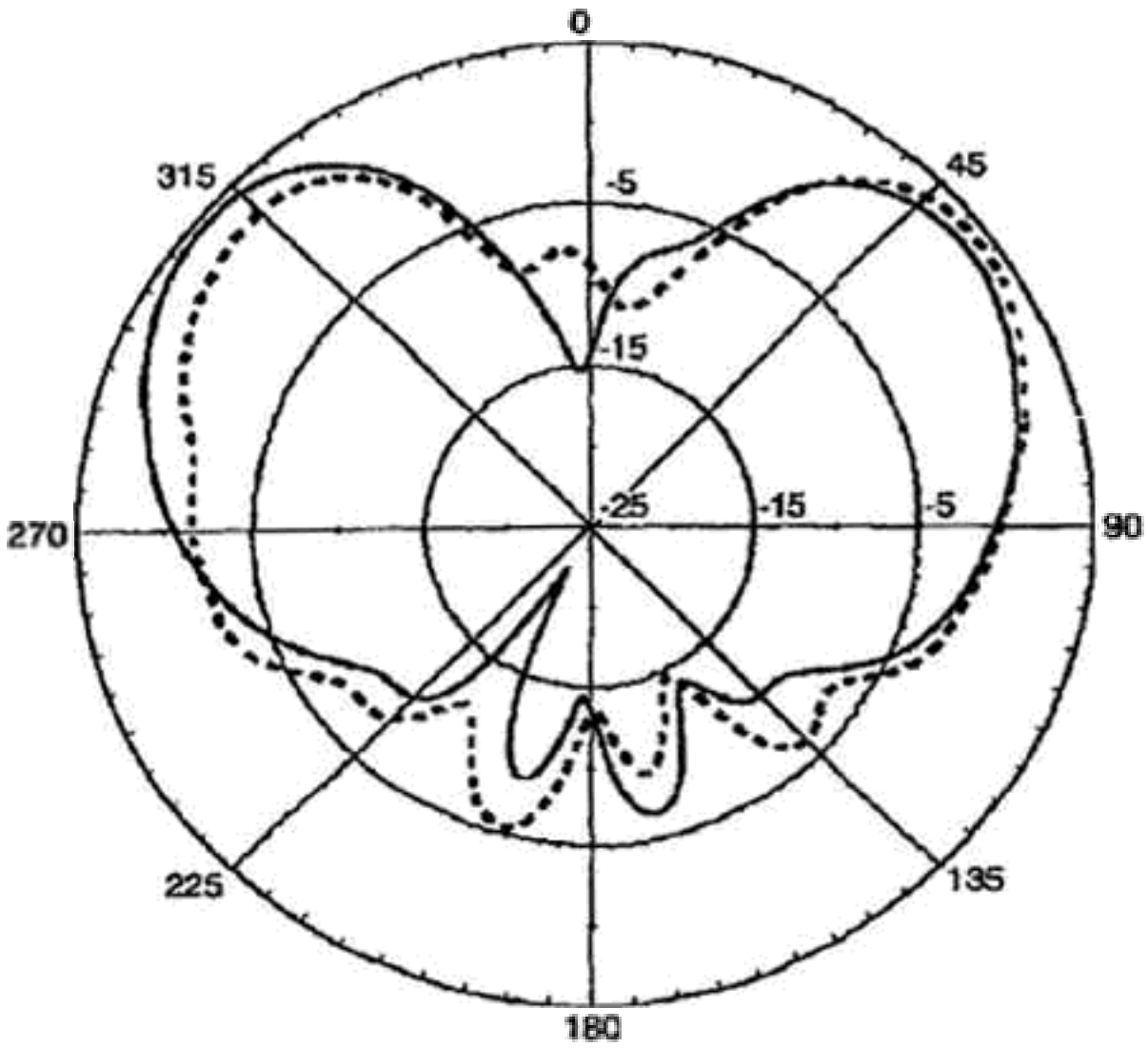

13.38 Measured radiation patterns of the antenna of Figure 13.37. — plane, —— H plane. (From [20] © 1998 I printed with permission.)

in Figure 13.38. The measured gain was 3.9 dBi across the relevant band of frequencies.

13.4 roiect~

. Design a rectangular patch with shorting pin at 5 GHz. Air substrate is used. Assume infinite ground plane. For your design, list the following parameters:

- Dimensions of the patch in centimeters and in units of wavelength at 5 GHz;
- Thickness of air substrate in centimeters and in units of wavelength t 5 GHz;
- Location of the shorting pin;
- Diameter of the shorting pi··

or your design, obtain (a) the VSWR versus frequency curve and determine its impedance bandwidth; (b) the co-polarization and cross polarization patterns at 5 GHz and at the frequencies f_2 and f_1, which are the upper and lower frequencies at which the VSWR = 2, respectively.

2. Design a U-slot rectangular patch with shorting wall at 5 GHz. Air substrate is used. Assume infinite ground plane. For your design, list the following parameters:

   - Dimensions of the patch in centimeters and in units of wavelength at 5 GHz;
   - Thickness of air substrate in centimeters and in units of wavelength at 5 GHz;
   - Dimensions and locations of the U-slot patch and show it in a diagram.

   For your design, obtain (a) the VSWR versus frequency curve and determine its impedance bandwidth; (b) the co-polarization and cross polarization patterns at 5 GHz and at the frequencies f_2 and f_1, which are the upper and lower frequencies at which the VSWR=2, respectively.

References

[1] Munson, "Microstrip Antenna" in R.C. Johnson and H. Jasik (Eds): *Antenna Engineering Handbook*, McGraw-Hill, New York, 1984, Chapter 7.

[2] S. Pinhas and S. Shtrikman, "Comparison between computed and measured bandwidth of quarter-wave microstrip radiators," *IEEE Trans. Antennas and Propagation*, Vol. AP-36(11), pp. 1615–1616, 1988

[3] R. Chair, K. F. Lee and K. M. Luk, "Bandwidth and cross-polarization characteristics of quarter-wave shorted patch antenna," *Microwave and Optical Technology Letters*, Vol. 22, No. 2, pp. 101–103, 1999.

[4] K. F. Lee, Y. X. Guo, J. A. Hawkins, R. Chair and K. M. Luk, "Theory and experiment on microstrip patch antennas with shorting walls," *IEE Proc.-Microwave, Antennas and Propagation*, Vol. 147, No. 6, pp. 521–525, 2000.

[5] K. Hirasawa and M. Haneishi, (Eds): "Analysis, design, and measurement of small and low-profile antennas," (Artech House, 1992), pp. 73–7..

[6] B. Waterhouse, S. D. Targonski, and D. M. Kokotoff, "Design and performance of small printed antennas," *IEEE Transactions on Antennas and Propagation*, Vol. 46, No. 11, pp. 1629–1633, 1998

[7] K. M. Luk, R. Chair and K. F. Lee, "Small rectangular patch antenna," *Electronics Letters*, Vol. 34, pp. 2366–2367, 1998

[8] R. Chair, K. M. Luk and K. F. Lee, "Small dual patch antenna," *Electronics Letters*, Vol. 35, No. 10, pp. 762–764, 1999.

[9] R. Chair, K. M. Luk and K. F. Lee, "Miniature multilayer shorted patch antenna," *Electronics Letters*, Vol. 36, No. 1, pp. 3–4, January 2000.

[10] R. Chair, K. M. Luk and K. F. Lee, "Novel miniature shorted dual-patch antenna," *IEE Proceedings-Microwave, Antennas and Propagation*, Vol. 137, pp. 273–276, 2000

[11] . Shackelford, K. F. Lee and K. M. Luk, "Design of small-size wide-bandwidth microstrip patch antennas," *IEEE Antennas and Propagation Magazine*, Vol. 45, No. 1, pp. 75–83, February 2003.

[12] Y. X. Guo, A. Shackelford, K. F. Lee, and K. M. Luk, "Broadband quarter-
:ch antenna with a U-shaped slot," *Microwave and Optical Technology Letters*, Vol. 28, pp. 328–330, 2001.

[13] A. K. Shackelford, K. F. Lee, K. M. Luk and R. Chair, "U-slot patch antenn
.vith shorting pin," *Electronics Letters*, Vol. 37, No. 12, pp. 729–730, June 2001

[14] A. A. Deshmukh and G. Kumar, "Half U-slot loaded rectangular microstrip antenna," in *IEEE AP-S Int. Symp.* USNC/CNC/URS National Radio Science Meeting, Vol. 2, pp. 876–879, 2003.

[15] T. Huynh and K. F. Lee, "Single-layer single-patch wideband microstrip antenna," *Electronics Letters*, Vol. 31, No. 16, pp. 1310–1312, 1995.

[16] C. L. Mak, R. Chair, K. F. Lee, K. M. Luk and A. A. Kishk, "Half U-Slo· patch antenna with shorting wall," *Electronics Letters*, Vol. 39, No. 25 pp.1779–1780, December 2003.

[17] R. Chair, K. F. Lee, C. L. Mak, K. M. Luk and A. A. Kishk, "Miniature Wide-band Half U-Slot and Half E-Shaped Patch Antennas," *IEEE Transactions on Antennas and Propagation*, Vol. 53, No. 8, pp. 2645–2652, Augus 2005

[18] L. Zaid, G. Kossiavas, J-Y Dauvignac, J. Cazajous, and A. Papiernik, "Dual-Frequency and broad-band antennas with stacked quarter wavelength elements," *IEEE Transactions on Antennas and Propagation*, Vol. 47, No. 4, pp. 654–660, 1999.

[19] R. B. Waterhouse, J. T. Rowley, and K. H. Joyner, "Stacked shorted patch antenna," *Electronics Letters*, Vol. 34, pp. 612–614, 199.

[20] R. B. Waterhouse, "Broadband stacked shorted patch," *Electronics Letters*, Vol. 35, No. 2, pp. 98–100, 1999.